Liquid Immiscibility in Silicate Melts and Related Systems

Article *in* Reviews in Mineralogy and Geochemistry · July 2007

DOI: 10.2138/rmg.2007.65.4

CITATIONS
58

READS
1,342

3 authors, including:

Alan Bruce Thompson
ETH Zurich
154 PUBLICATIONS **12,727** CITATIONS
SEE PROFILE

Alistair Hack
The University of Newcastle, Australia
31 PUBLICATIONS **1,006** CITATIONS
SEE PROFILE

Reviews in Mineralogy & Geochemistry
Vol. 65, pp. 99-127, 2007

Liquid Immiscibility in Silicate Melts and Related Systems

Alan B. Thompson*, Maarten Aerts, Alistair C. Hack

Dept. Erdwissenschaften, ETH Zürich
Institute for Mineralogy & Petrology
Clausiusstrasse 25
Zürich, CH-8092, Switzerland

**also at Faculty of Mathematics and natural Sciences, University of Zürich, Switzerland*
alan.thompson@erdw.ethz.ch maarten.aerts@erw.ethz.ch alistair.hack@erdw.ethz.ch

INTRODUCTION TO NATURAL IMMISCIBLE SYSTEMS

High temperature melts, fluids and gases progressively organize themselves structurally during cooling, usually causing separation of solids, liquids or gases. In many different chemical systems this phase separation results in distinct chemical separation (*immiscibility*), with associated contrasting physical properties in the separating phases. Because of the variety in chemistries, and relative changes in entropy and volumes of the natural mixtures compared to the separated phases, immiscibility can occur in different chemistries during heating and compression, as well as during cooling and decompression.

Although the main emphasis in this volume is on fluid–fluid equilibria, there are good examples and much literature on liquid–liquid equilibria in synthetic silicate melts and natural magmas. In fact much of our understanding of phase separation (for geochemists generally taken simply as liquid–vapor equilibria) actually originates from liquid–liquid immiscibility studies of silicate melts. For a one-component system there are three distinct regions in *PT* space where either solid or liquid or vapor exist as the stable phase. These are separated by three univariant curves (i) the solid–liquid curve, the solidus, (ii) the liquid–vapor curve, which can lead to the most commonest form of critical point (see Fig. 1a), and (iii) the solid–vapor curve, which reflects direct vaporization (sublimation) or condensation of solids from gas. The latter is relevant in some industrial processes and to condensation of stars at vacuum pressures. For each added component with solid, liquid and vapor phases, there is the possibility of mixing of each of the phases, or not. In silicates we are used to recognize immiscibility gaps (solvus) among chemically related minerals (e.g., alkali feldspars), which are miscible at high temperatures in the subsolidus region but are immiscible with cooling and undergo phase separation. We are less used to consider immiscibility between two anhydrous melts (silicate–silicate, silicate–carbonate, silicate–oxide, silicate–sulfide, etc.).

The occurrence of liquid immiscibility in temperature–composition (*T–X*) diagrams is represented by the crest of a two liquid (L_1–L_2) solvus lying at higher temperatures than the melting curve, which it intersects at a eutectic or peritectic (Figs. 1 and 2). By changing chemistry and pressure, it can be observed that the L–L solvus can occur at lower temperature. It appears to pass through the liquidus and in some cases can occur only metastably below the liquidus (Figs. 1e, 2a,b,c). The liquidus region here consists of *supercritical melt*. So the definitions of whether systems are immiscible (Fig. 2), miscible, supersolvus or supercritical depend upon the relative intersections of two curves, the solidus and the *P–T* trajectory of the solvus (critical curve). There are continuous changes in physical properties with chemical composition through critical points. In some liquid–gas systems (also in nature) there are

1529-6466/07/0065-0004$05.00 DOI: 10.2138/rmg.2007.65.4

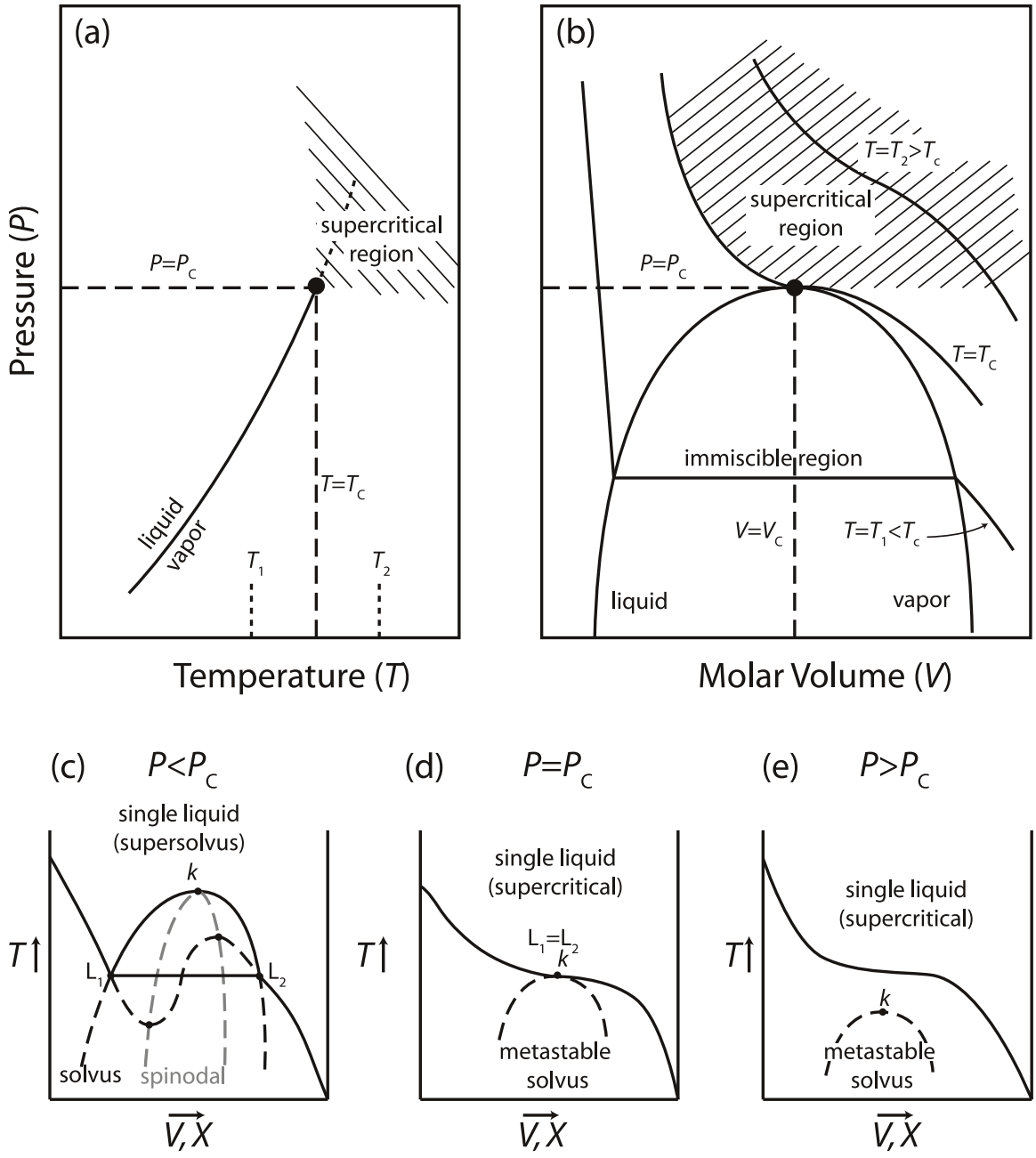

Figure 1. Pressure (P) – Temperature (T) – Volume (V) relations for simple systems showing immiscible, supersolvus and supercritical melt or fluid. (a) P–T diagram for a one component system showing the liquid-vapor equilibrium curve extending to the critical point (where P=P_c, T=T_c). At higher P and T than this, the single phase is the supercritical fluid. (b) P–V section for a one component (or P–X in a two-component) system with three isotherms, showing how immiscible liquid and vapor are distinct (where (T=T_1<T_c). These phases are identified by quite different compositions in a binary join, with quite different physical properties (e.g., volume here, but could be density, enthalpy, etc.). P–V and T–V sections for one component fluid have similar form, but can even have opposite slope depending upon the dP/dT of the critical curve, (e.g., Levelt Sengers 2000). (c-e) Three T–X sections for a two component binary system at different pressures showing relations between solvus and solidus, (c) below P_c, (d) at P_c, (e) above P_c. The components could be oxide–SiO_2 in anhydrous systems, or rock–H_2O as discussed by Hack et al. (2007) . Note the metastable extensions of the solidus curve in (c) inflect at the spinodal (see Prigogine and Defay 1954, p.231).

some important changes expected when circulating in *P–T* in specific directions near to critical compositions (e.g., see Stanley 1971; Hack et al. 2007). But there are probably no rapid changes (spectacular phenomena) involving criticality alone, to be expected in rock+melt systems along common *PT* paths inside the Earth (at least not so far). In recent years there have been considerable advances on studying immiscibility in anhydrous molten silicate systems, but not all in the geological literature. We have not attempted to review the complete developments contained in other recent reviews mentioned here, but rather to integrate these new results into the two silicate melt situation.

Immiscible anhydrous silicate melts and magmas

Immiscible silicate melts have been of interest in geological sciences at least since the late 19th century (see Rosenbusch 1872), when nearby rocks of quite different chemical composition (notably rhyolite and basalt) were suggested to have formed by splitting of an intermediate composition into two-immiscible magmas. In the 1920's, experiments by Greig (1927a,b) and by Bowen (1928) suggested that the liquid immiscibility of binary silicate systems did not extend far into the natural range of rock compositions.

However, natural unmixing of anhydrous silicate melts is still considered to be responsible for a variety of natural rock associations (some mid-oceanic ridge basaltic (MORB) magmas, anorthosites, lunar and terrestrial tholeiitic to alkaline basaltic volcanics, lamprophyre dykes in granitoids, and some layered intrusions; see summary by Roedder 1978). Observations on natural silicate glasses and quenched melts are now complemented by a vast experimental and theoretical literature on liquid immiscibility in technological silicate melts and glasses. Systematic experimental studies of molten oxide-SiO_2 binary systems showed that two immiscible melts can occur in some cases. One very silica-rich melt (often labeled L_1 as in Fig. 1c, SiO_2 on the left; e.g. Barth 1962, p. 144) coexists with a second melt of intermediate composition, usually L_2 (as in Fig. 1c). In other cases, the two-immiscible melts occur only metastably below (at lower temperature than) the liquidus or even solidus. This reflects a transition from immiscible to supercritical melt behavior with increasing pressure or as a function of composition, as discussed further below. The meaning of the term liquidus is quite clear and separates the all melt region from that with solids. The meaning of the term solidus is less clear and is used to refer to the first signs of melt along a divariant melting loop or to a eutectic in binary or higher-degree systems, as well as to the univariant curve for pure substances in the *PT*-diagram (where solidus and liquidus are identical).

LIQUID IMMISCIBILITY IN SILICATE MELTS

Glassy globules of distinct mafic and felsic compositions in tholeiitic to alkaline basaltic rocks (Freestone 1978; Biggar 1979; Dixon and Rutherford 1979; Philpotts 1982; Phillpotts and Doyle 1983; Jakobsen et al. 2005) and ocelli in lamprophyre dykes (felsic blobs in a mafic matrix) are examples (Philpotts 1976; Foley 1984; Bedard 1994) of suggested immiscibility in low pressure volcanic rocks. Most evidence for liquid immiscibility in higher pressure plutonic rocks is much less convincing (e.g., see summary by Bogaerts and Schmidt 2006).

Silicate-oxide anhydrous molten binary systems and the role of network-forming and network-modifying cations

SiO_2 (silica)-rich melts are very viscous and easily suited to glass-working because during cooling they do not quench readily to crystals. It has been shown (e.g., papers in Stebbins et al. 1995) that such siliceous melts consist of a polymeric network of SiO_2, barely modified by additional oxides. Further addition of such oxides eventually (in some cases after passing through a two-liquid region) results in melts of much lower viscosity, where the additional oxides have severely modified the SiO_2-network. Kracek (1930, 1932) summarized the melting

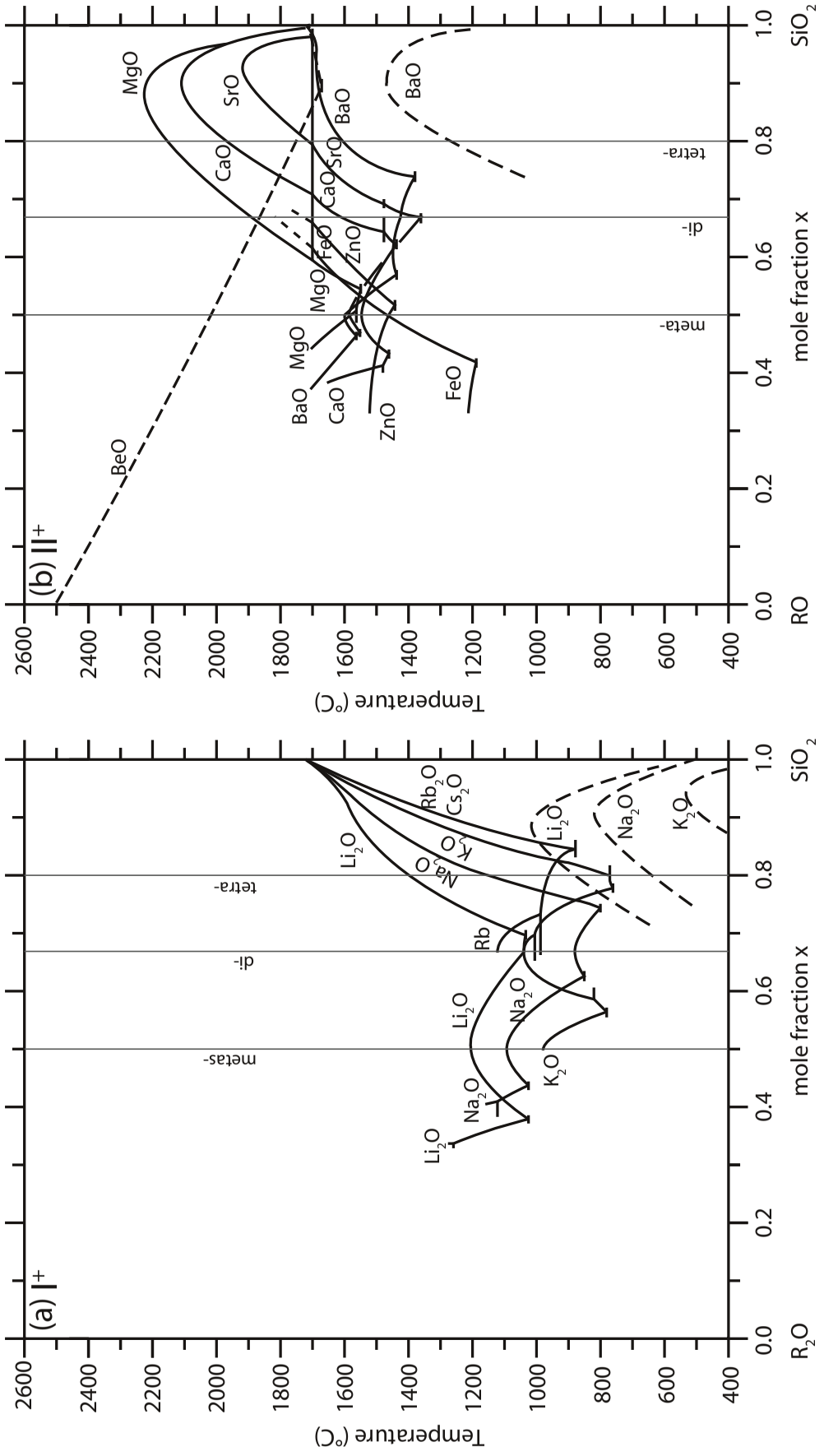
(b) II+
(a) I+
Temperature (°C)
mole fraction x
RO
R2O
SiO2
tetra-
di-
meta-
metas-
BeO
MgO
SrO
CaO
BaO
FeO
ZnO
Li2O
Na2O
K2O
Rb2O
Cs2O
Rb

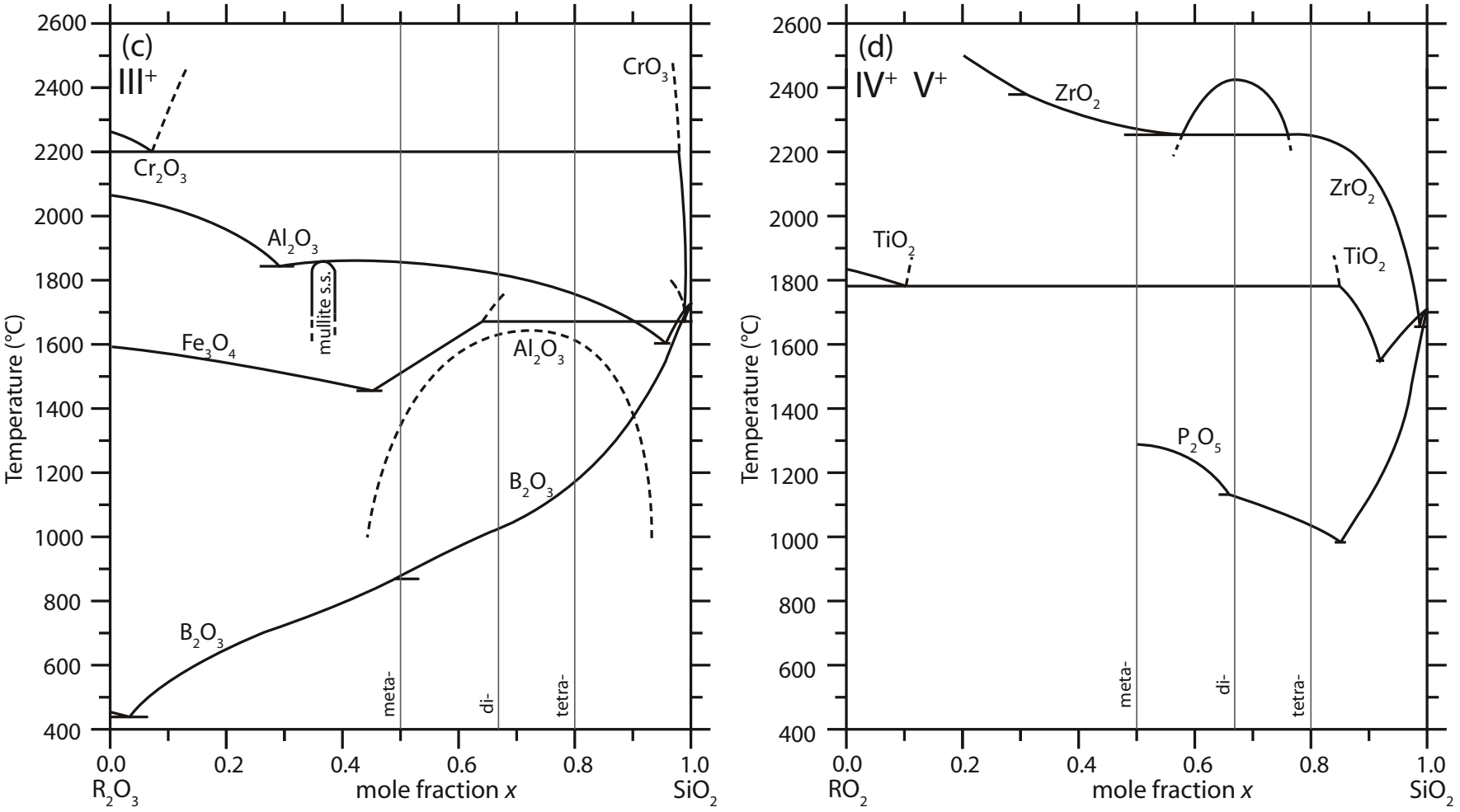

Figure 2. Liquidus temperature-composition diagrams for: (a) 1^+ oxide–silica binaries. The liquidus data were first summarized by Kracek (1930, 1932) and presented in *Phase Diagrams for Ceramists* (Levin et al. 1964, Fig. 128; see also Veksler 2004 , p. 12). We have added recent subsolidus data on submerged solvi (see Table 1 for references). (b) 2^+ oxide–silica binaries (data in Table 1). (c) 3^+ oxide–silica binaries (data in Table 1). Note that Fe_3O_4–SiO_2 is not a true binary but an isobaric section through the system FeO–Fe_2O_3–SiO_2 in air at 1 atm (see Phillips and Muan 1959) (d) 4^+ and 5^+ oxide–silica binaries (data in Table 1). The stoichiometries for silicate compounds on a molar basis with examples for Na_2O–SiO_2 are according to Kracek (1930, 1932): ortho- (2:1, Na_4SiO_4); meta- (1:1, Na_2SiO_3); di- (1:2, $Na_2Si_2O_5$); tetra- (1:4, $Na_2Si_4O_9$).

diagrams of several oxide–silica binary systems in temperature–composition (T–x, SiO_2 on the right) diagrams. His original figures have been used, and added to, by several authors (see Table 1 and Figs. 2a to 2d)

The 1^+-oxides with SiO_2 show steepening of the slope of the liquidus and the movement of the composition of the first eutectic towards higher-SiO_2 in the order Li > Na > K > Rb > Cs (towards heavier/larger atoms). Recent studies (Table 1) have located the metastable two-liquid regions (identified by onset of opalescence for different prepared glass compositions, Fig 2a), with T_c (critical temperature, L_1=L_2) decreasing and X_c (critical composition) moving towards SiO_2 in the order Li > Na > K (Fig. 2a).

The T–x diagrams for 2^+-oxides with SiO_2 (Fig. 2b) show clearly two-immiscible melts (liquids), with one composition being very close to SiO_2 (L_1) and the other at intermediate compositions towards the oxide (L_2). The phase diagram includes a peritectic reaction with cristobalite (the high-temperature polymorph of SiO_2), and upon cooling the reaction of siliceous liquid (L_1) to cristobalite and the intermediate composition liquid (L_2) occurs (the peritectic reaction $L_1 = SiO_2 + L_2$). T_p is used to denote the temperature of such a peritectic reaction, where upon cooling one phase reacts to two phases. There is a distinct migration of the composition of L_1 towards SiO_2, and the decreasing temperature of the top of the two-liquid region (the critical temperature of the solvus, T_c), from Fe > Mg > Ca > Sr > Ba (i.e., towards heavier/larger atoms).

Table 1. References for melting equilibria in binary systems with SiO_2

I^+		II^+		II^+, VI^+, V^+	
Li_2O	Kim and Sanders 1991 Kracek 1930 Samsonov 1982 Moriya et al. 1967	**BeO**	Morgan and Hummel 1949 Budnikov and Cherepanov 1953	**Cr_2O_3**	Bunting 1930 (b)
Na_2O	Kim and Sanders 1991 Kracek 1930 Samsonov 1982 Haller et al. 1974	**MgO**	Wu et al. 1993 Michels and Wesker 1988 Ol'shanskii 1951 Kracek 1930	**Fe_2O_3**	Phillips and Muan 1959
K_2O	Kim and Sanders 1991 Kracek 1930 Moriya et al. 1967 Kawamoto and Tomozawa 1981 Samsonov 1982	**CaO**	Hageman et al. 1986 Hageman and Oonk 1986 Ol'shanskii 1951 Kracek 1930 Tewhey and Hess 1979 Taylor and Dinsdale 1990	**Al_2O_3**	MacDowell and Beall 1969 Staronka et al. 1968 Davis and Pask 1972 Aramaki and Roy 1962 Ball et al. 1993
Rb_2O	Kim and Sanders 1991 Kracek 1930 Alekseeva 1963	**SrO**	Huntelaar et al. 1993 Fields et al. 1972 Ghanbari and Brett 1988 (a, b) Ol'shanskii 1951 Kracek 1930	**TiO_2**	Kaufman 1988 DeVries et al. 1954
Cs_2O	Kim and Sanders 1991 Kracek 1930 Samsonov 1982 Charles 1966	**BaO**	Seward et al. 1968 (a, b) Kracek 1930 Ol'shanskii 1951	**ZrO_2**	Ball et al. 1993 Butterman and Foster 1967
		ZnO	Bunting 1930 (a, c)	**MnO_2**	Singleton et al. 1962 Glasser 1958 White et al. 1934
		FeO	Wu et al. 1993 Bowen and Schairer 1932	**P_2O_5**	Tien and Hummel 1962 Baret et al. 1991 Ryerson and Hess 1980

Figure 2c shows SiO_2 binaries with 3^+-oxides (Al_2O_3, Fe_2O_3, B_2O_3, Cr_2O_3), and Figure 2d the 4^+ oxides (TiO_2, ZrO_2) and a 5^+ oxide (P_2O_5) with SiO_2. In summary, relative to the 2^+-oxides–SiO_2 systems which show extensive two-liquid immiscibility, the 1^+-oxide–SiO_2 systems show increasing supercriticality with atomic number; the 3^+ oxide Al_2O_3–SiO_2 and the 5^+ oxide P_2O_5–SiO_2 do not show immiscibility because of compound formation (mullite at $3Al_2O_3{\cdot}2SiO_2$; and $P_2O_5{\cdot}SiO_2$, $2P_2O_5{\cdot}3SiO_2$, $P_2O_5{\cdot}4SiO_2$) whereas Fe_2O_3–SiO_2, then Cr_2O_3–SiO_2, as well as TiO_2–SiO_2, ZrO_2–SiO_2, show extensive and progressively increasing L–L immiscibility towards higher temperatures.

High melting point compounds break up the composition join in some cases. Immiscibility is evidence that intermediate compounds of any state (S, L or V) are not stable over the immiscible range. Intermediate solid compounds limit the range over which L–L immiscibility can occur and establish eutectic, peritectic or minimum melting relations. Where intermediate compounds are stable, immiscibility is suppressed. These relations can be seen comparing the relative prevalence of intermediate compounds and immiscibility, compare 1^+ and 5^+ (P_2O_5) oxide–silica versus 2^+, 3^+, 4^+ oxide–silica (Fig. 2).

Factors controlling immiscibility or supercriticality in anhydrous silicate-oxide binary molten systems

The critical (or consolute) temperatures (T_c) of the two-melt fields observed in *T–X* melting diagrams (as noted with regard to Figs. 1 and 2), appear to correlate with Coulombic properties of the metal cations, such as ionic potential—the ratio of Z/r, where Z is the nominal charge and r is the atomic radius (Fig. 3a,b; see reviews by Hess 1980, 1995; Hudon and Baker 2002a; Veksler 2004; and references therein).

Veksler (2004) made a summary of Hess's (1995) conclusions, here paraphrased: the correlation between T_c and Z/r (Hess 1996, p. 2373, Fig. 9) can be viewed as an indication that the main forces at the atomic scale responsible for the phase separation are Coulombic in character and repulsive. In this view, bridging oxygen ions of highly polymerized silica networks provide poor shielding of network-modifying cations, which results in substantial Coulombic repulsions between the cations, and may eventually lead to phase separation. The higher the ionic potential of modifier cations, the greater are the Coulombic repulsions between them, and the larger are the two-liquid fields in oxide–silica binaries.

However, the detailed examination of liquid immiscibility phenomena in the mineral-silica binaries by Hudon and Baker (2002a,b), revealed more complex relationships between ionic potentials and *T–X* dimensions of the liquid–liquid miscibility gaps, and were summarized by Veksler (2004, p. 13), here paraphrased: Hudon and Baker (2002a,b) proposed that other factors, mostly related to configurations of electron shells of ions, affected liquid immiscibility. A plot of the critical (consolute) temperatures versus Z/r (Z, r are defined two paragraphs above) constructed by Hudon and Baker (2002a,b; here Fig. 3a) demonstrates that the relationships are parabolic, not linear. Homovalent cations (mono-, di-, trivalent, etc.) can be fitted each by a separate parabola. In relation to two-liquid immiscibility, Hudon and Baker (2002a,b) subdivided cations into four groups. The first group includes large cations (r > 87.2 pm in octahedral coordination), which have coordination numbers 5 and higher, cannot enter tetrahedral sites and can act in melt structures only as network modifiers. The typical representatives of the group are alkalis from Na to Cs, alkaline earths from Ca to Ba, light rare-earth elements, U and Th. The second group consists of amphoteric cations (e.g., Li^+, Mg^{2+}, Ga^{3+}, Al^{3+}, Ti^{4+} and Nb^{5+}), which have ionic radii larger than that of Si^{4+} (26 pm, Shannon 1976) but smaller than about 87.2 pm in six-fold coordination or 78.6 pm in four-fold coordination. Bonds formed by those cations with O^{2-} are characterized by substantial degree of covalency. This results in a better shielding of the cations and lower critical (consolute) temperatures than expected from the Z/r values. The third group includes cations with variable crystal field stabilization energies (commonly abbreviated VCFSE). They are formed by

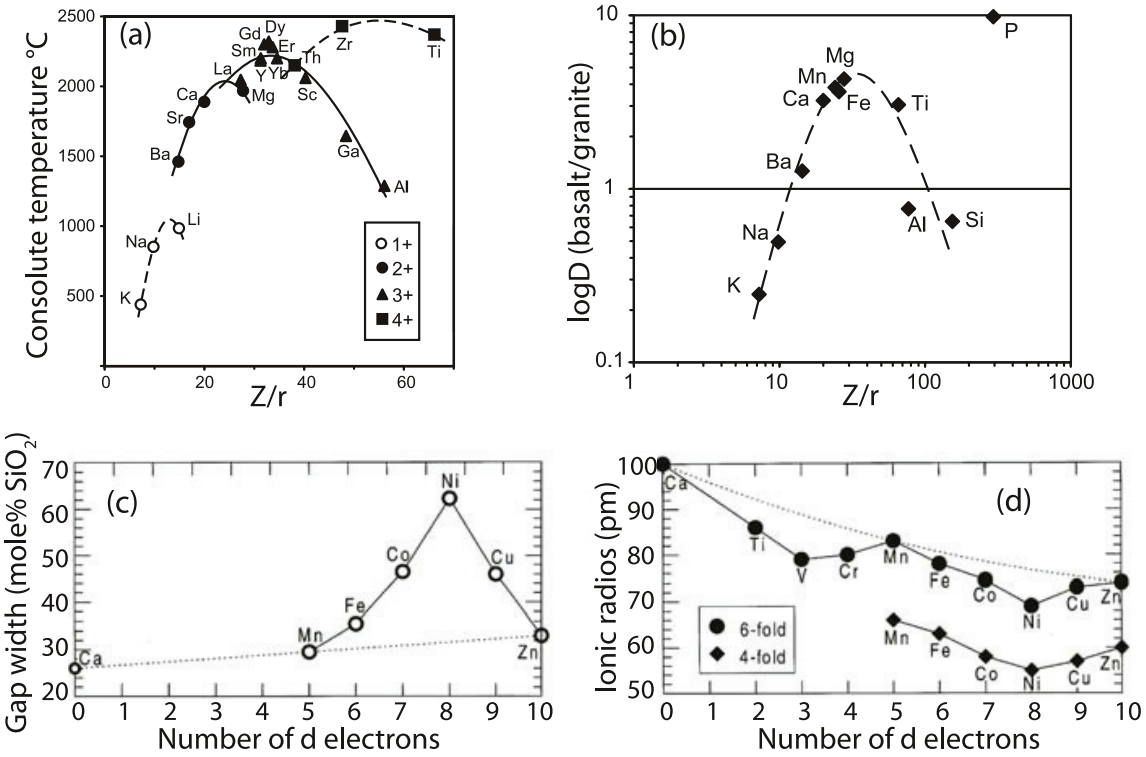

Figure 3. Effects of network-modifying cations on liquid immiscibility in anhydrous silicate systems (a) Consolute (critical) temperatures of the miscibility fields in the metal oxide – silica binaries as a function of the Coulombic properties of the metal cations (after Hudon and Baker 2002a,b); (b) Partitioning coefficients (D) of elements between anhydrous immiscible ferrobasaltic and granitic melts at atmospheric pressure, from experimental data by Longhi (1990) and Ryerson and Hess (1978). Dashed curve is a reference curve emphasizing the general trend of the data points, plotted as *Z*/*r*; *Z*—nominal electric charge, *r*—ionic radii in nanometers from Shannon (1976), see Veksler (2004) for discussion [Used by permission from Elsevier, from Veksler (2004), *Chemical Geology*, Vol. 210, Fig. 3, p. 14]; (c) miscibility gap widths of divalent cations with variable crystal field stabilization energies (VCFSE), and (d) Ionic radii of divalent cations with VCFSE. Cations adopting a low-spin state are expected to have very large immiscibility fields. The miscibility gap widths of Mn^{2+} and Ni^{2+} are assessed from the main trend defined by Hudon and Baker (2002a) [Used by permission from Elsevier, from Hudon and Baker (2002), *J Non-Cryst Solids*, Vol. 303, Fig. 5, p. 323].

elements that occupy the first row of transition elements in the periodic table (Fe^{2+}, Co^{2+}, Ni^{2+}, Cu^{2+}, V^{2+} and Cr^{2+}) and characterized by five *d*-electron orbitals. The orbitals are known to poorly shield the atomic nucleus (Hudon and Baker 2002a,b; and references therein), and the miscibility gaps associated with the cations in the binaries are larger than expected from simple *Z*/*r* relationships. Finally, highly polarizable cations with a lone pair of electrons (Pb^{2+}, Sn^{2+}, Bi^{3+}, Tl^{2+} and Te^{4+}) show better compatibility with polymerized silica-, borate- and germanate-networks and reduced miscibility gaps (Hudon and Baker 2002b).

Effect of higher pressure on liquid immiscibility in anhydrous molten silicate binaries

Although high pressure–temperature melting experiments have been conducted for some time (Bridgman 1927; Boyd and England 1960; see papers in Hemley 1999; and Hazen and Downs 2001) only recently has attention been focused on the anhydrous silicate binaries. From their experiments on MgO–SiO_2, CaO–SiO_2 and $CaMgSi_2O_6$–SiO_2, Hudon et al. (2004) have shown (Fig. 4a,c) that the critical curve (the *P,T* locus of the critical temperatures, T_c, where L_1=L_2) has a positive d*P*/d*T* slope (i.e., moves to higher *T* with increasing *P*). Moreover, because the peritectic reaction SiO_2-mineral+L_2=L_1 (at T_p) has a positive d*P*/d*T* slope that is

less steep than the critical curve, the two curves intersect at higher pressure. This is shown in Figures 4a and 4c. This point shows the pressure where both T_c and T_p occur at the same temperature ($T_c = T_p$), it is a critical point. At lower pressures $T_c > T_p$, and at higher pressures $T_c < T_p$. The progress towards supercriticality, involves moving through the intersection (where $T_c = T_P$) of the critical curve and liquidus for the binary which is represented by the peritectic reaction, SiO_2-mineral+L_2=L_1. The SiO_2 liquidus becomes supercritical at $P \geq P$ ($T_c = T_P$), because the L_1+L_2 solvus submerges below the liquidus and becomes metastable. Hudon et al. (2004, page 12) suggest that the two liquid miscibility gaps close at 1.81 ($MgO–SiO_2$) and 1.33 GPa ($CaMgSi_2O_6–SiO_2$). Dalton and Presnall (1997) also suggested that $MgO–SiO_2$ becomes supercritical below 5.0 GPa. Figures 4a and 4b suggest that the $MgO–SiO_2$ L_1+L_2 miscibility gap is metastable (i.e., liquids are supercritical) above ca. 2 (± 0.2) GPa and that $CaMgSi_2O_6–SiO_2$ is supercritical at pressures above ca. 1.5 (± 0.2) GPa.

Hudon et al. (2004, p.14) and Hudon and Baker (2002a,b) noted that for silica-1^+oxide binaries, increasing pressure beyond P_c further decreases the size of the metastable miscibility gaps (example $Li_2O–SiO_2$), i.e. promotes supercriticality. For Ti^{4+} in $TiO_2–SiO_2$, pressure enlarges the size of immiscibility fields (experiments at 3 GPa by Circone and Agee 1995). Hudon et al. (2004, p.14, § 42) explain this as follows "Pressure appears to have a more pronounced effect on Ti^{4+} than on Mg^{2+} or Li^+, because there is probably more Ti^{4+} than Mg^{2+} or Li^+ in four-fold coordination in binary melts. Consequently, increasing pressure converts more Ti^{4+} than Mg^{2+} or Li^+ to six-fold coordination, which enlarges the $TiO_2–SiO_2$ miscibility gap more than the immiscibility fields associated with Mg^{2+} or Li^+. This explanation is supported by the ionic potentials (defined as Z/r; where Z is the valence and r is the ionic radius) of the cations: IV-fold Ti^{4+} has the largest with 9.52, IV-fold Mg^{2+} has 3.51, and IV-fold Li^+ has the smallest with 1.69; consequently Ti^{4+} is the most capable of polarizing the oxygen anions toward it to make covalent bonds and adopt a coordination of 4 while Li^+ is the least." Their conclusions are illustrated in Figures 3c and 3d.

Simplified representations of immiscibility, miscibility and supercriticality

Taken all together, these binary (oxide–SiO_2) melting diagrams show a quite remarkable progression of decreasing immiscibility with higher charge and atomic numbers, through BaO–SiO_2 (Greig 1927a, his Fig. 13) where the liquidus has a small flat (S-shaped portion, Fig. 2b), through to the 1^+-oxides–silica where the liquidus is inflected (S-shaped) and hides the metastable 2-liquid region (Figs. 1e and 4b). *The passing of the critical point (T_c) of the 2-liquid region through the liquidus locates the supercritical point*. Thus, the *T–x* phase diagrams for 1^+-oxide–silica binaries all show supercritical melt (liquid) behavior. The *subcritical region* is where immiscibility occurs and two liquids are related through a peritectic reaction with the end-member solid, and the *supercritical melt region* occurs where there is a continuity of melt compositions from SiO_2- end-member to eutectic with a second solid. Such nomenclature is discussed further by Hack et al. (2007) in the context of liquid-gas-fluid systems. In all such systems the difference between the two phases can be seen by plotting against temperature (*T*), a chemical compositional variable (*T–X*), or a physical property (*T–V*, volume, *T–*ρ, density, *T–*η, viscosity, as in Fig. 1b).

TERNARY AND HIGHER ANHYDROUS MOLTEN SILICATE SYSTEMS

Consideration of the binary *T–x* diagrams in Figures 2 and 4 indicates which combination in ternary or higher systems will lead to extended immiscibility or not. These anticipations can be compared with the experimentally produced phase diagrams (e.g., the compilations called "*Phase Diagrams for Ceramists*" from the American Ceramic Society, since 1964, *http://www.acers.org/publications/phasecdform.asp*).

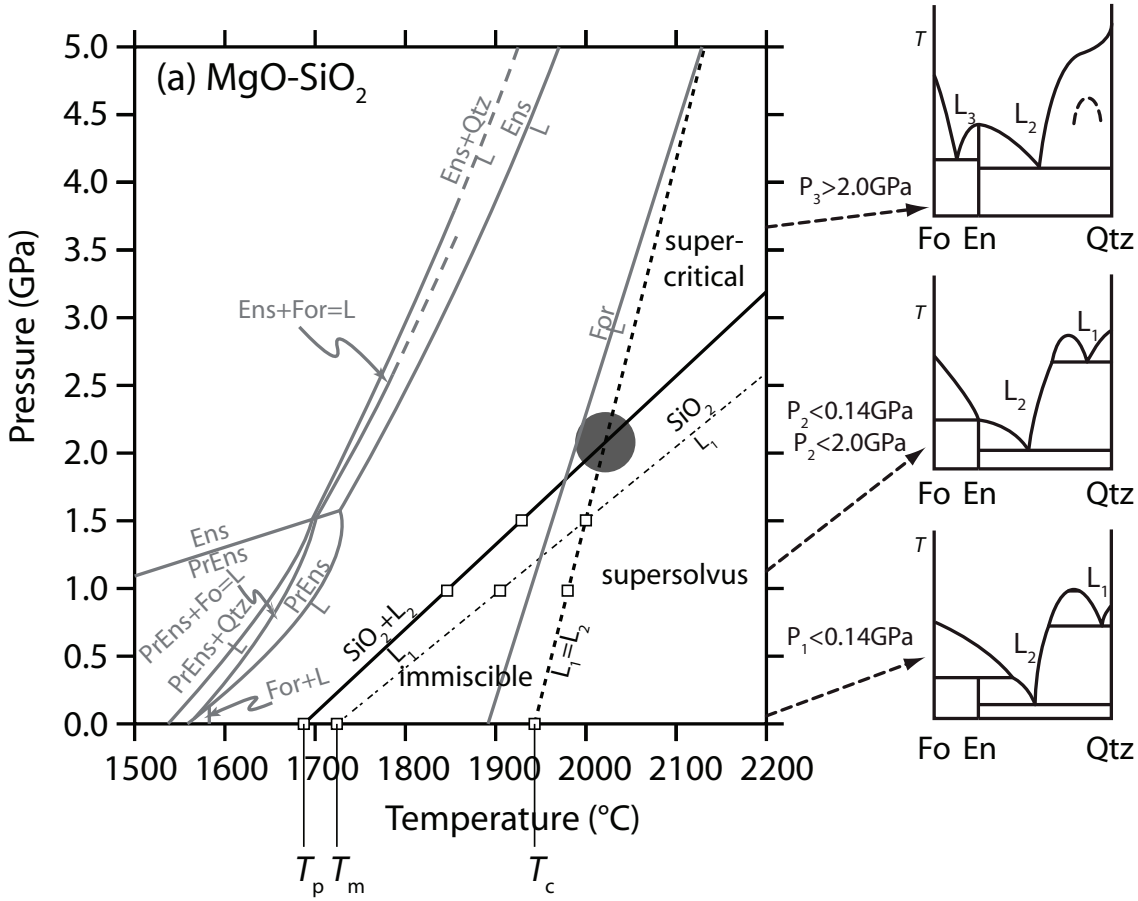
(a) MgO-SiO2
Pressure (GPa)
Temperature (°C)
Ens+Qtz
Ens
Ens+For=L
For
super-
critical
Ens
PrEns
PrEns+Fo=L
PrEns+Qtz
PrEns
For+L
SiO2+L2
L1
immiscible
L1=L2
SiO2
L1
supersolvus
Tp Tm
Tc
P3>2.0GPa
P2<0.14GPa
P2<2.0GPa
P1<0.14GPa
T
L3
L2
L1
Fo En
Qtz

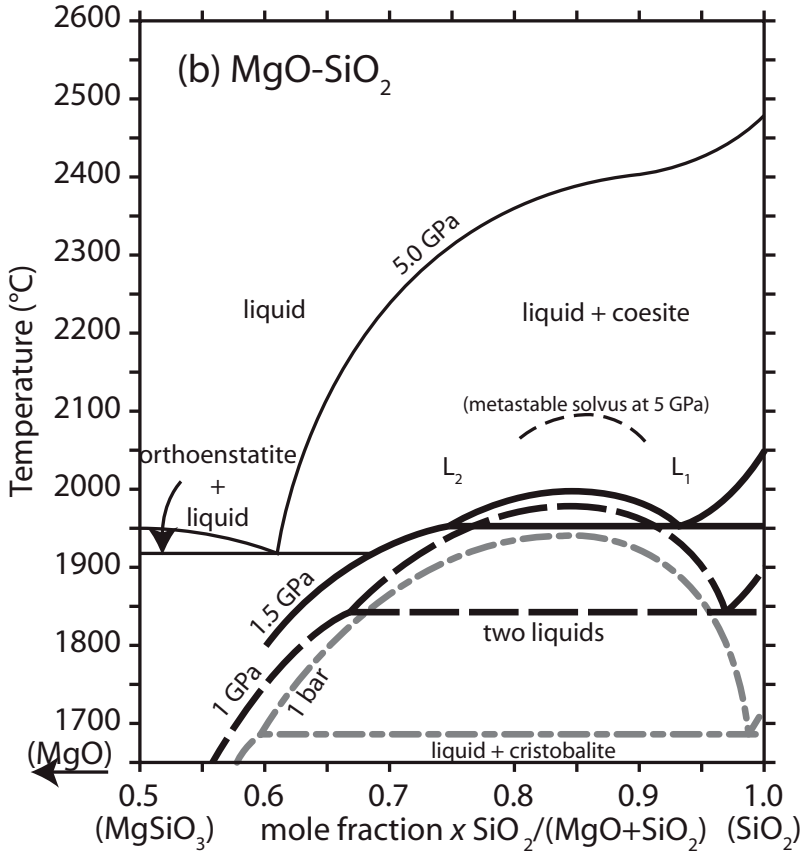
(b) MgO-SiO2
Temperature (°C)
5.0 GPa
liquid
liquid + coesite
(metastable solvus at 5 GPa)
orthoenstatite
+
liquid
L2
L1
1.5 GPa
1 GPa
1 bar
two liquids
liquid + cristobalite
(MgO)
(MgSiO3)
mole fraction x SiO2/(MgO+SiO2)
(SiO2)

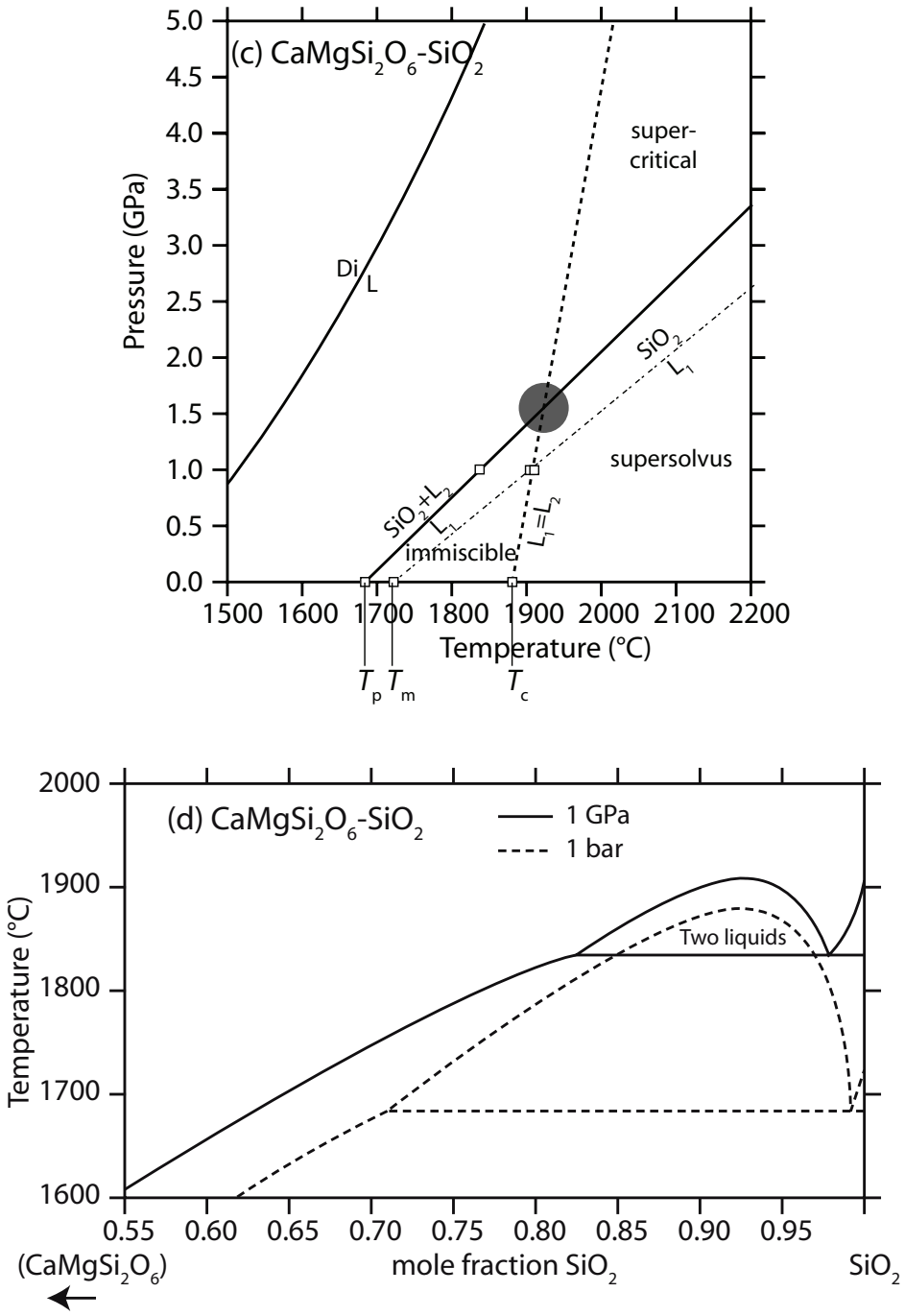

Figure 4 (*on facing page and above*). *P-T* and *T-x* diagrams for MgO–SiO_2 and $CaMgSi_2O_6$–SiO_2: (a) *P-T* diagram for Mg_2SiO_4–SiO_2 showing the +d*P*/d*T* for the melting curve of pure silica ($T_m SiO_2$), the critical curve for the two liquid region (T_c, where $L_1 = L_2$), and the labeled peritectics (T_P; on cooling, $L_1 = L_2 + SiO_2$-mineral). The intersections near 2000 °C, 1.5 GPa and 2020 °C, 2.1 GPa show respectively, the temperatures where $T_c = T_m SiO_2$, and the anticipated anhydrous critical end points (grey shaded region where $T_c = T_P$. Immiscible regions are distinguished from miscible regions (and distinguishing supersolvus from supercritical), as are supersolvus from supercritical. Reactions involving proto-enstatite (±quartz) and forsterite melting (lighter, grey curves) are adapted from Morse (1980, p. 363) using data of Boyd et al. (1964). Reactions Ens+For=L and PrEns+For=L from Chen and Presnall (1975), (b) *T-x* diagram for MgO–SiO_2 at several pressures superimposed, constructed from Morse(*) (1980, fig. 18.15 p. 362), from Hudon et al. (2004), with data at 5 GPa from Dalton and Presnall (1997), (c) *P-T* diagram for $CaMgSi_2O_6$–SiO_2, (d) *T-x* diagram for $CaMgSi_2O_6$–SiO_2, modified from Hudon et al. (2004), diopside liquidus from Boyd and England (1963). Open symbols at 1 atm, 1.0, and 1.5 GPa are data points from Wu et al. (1993), Jung (2003) and Hudon et al. (2004, Figs. 3 and 4). (*)*Note*: Morse (1980) in his Figure 18.15 (p. 362) shows Ens+For=L occurring at a lower *T* than Ens+Qtz=L. (a) is constructed according to the relative *P-T* positions for the reactions Ens+For=L and Ens+Qtz=L, as reported in Chen and Presnall (1975) and Boyd et al. (1964), respectively.

Two binaries both with immiscibility will produce an immiscibility tunnel across the ternary system (e.g., MgO–FeO–SiO_2, Bowen and Schairer 1935). Addition of a higher charge cation (e.g., Ti^{4+}) will extend the immiscibility of a 2^+-oxide–SiO_2 binary (e.g., TiO_2–MgO–SiO_2, Greig 1927a). Addition of a lower-charged cation (e.g., Li^+, Na^+) will decrease the immiscibility region of a 2^+-oxide–SiO_2 or higher system. These observations formed one of the original objections by Greig (1927b) to widespread silicate melt immiscibility in more complex systems compared to basic ternaries. Even though 2-liquid immiscibility is observed in many anhydrous silicate melting systems, they remain in compositions never, or only very rarely, found in nature. In Irvine's (1975b) synthesis of immiscibility effect in magmas, he noted that mafic binaries with silica maintained immiscibility, whereas felsic binaries with silica had eutectic and probably "submerged" critical phenomena (Fig. 5). Addition of anorthite (Andersen 1915;

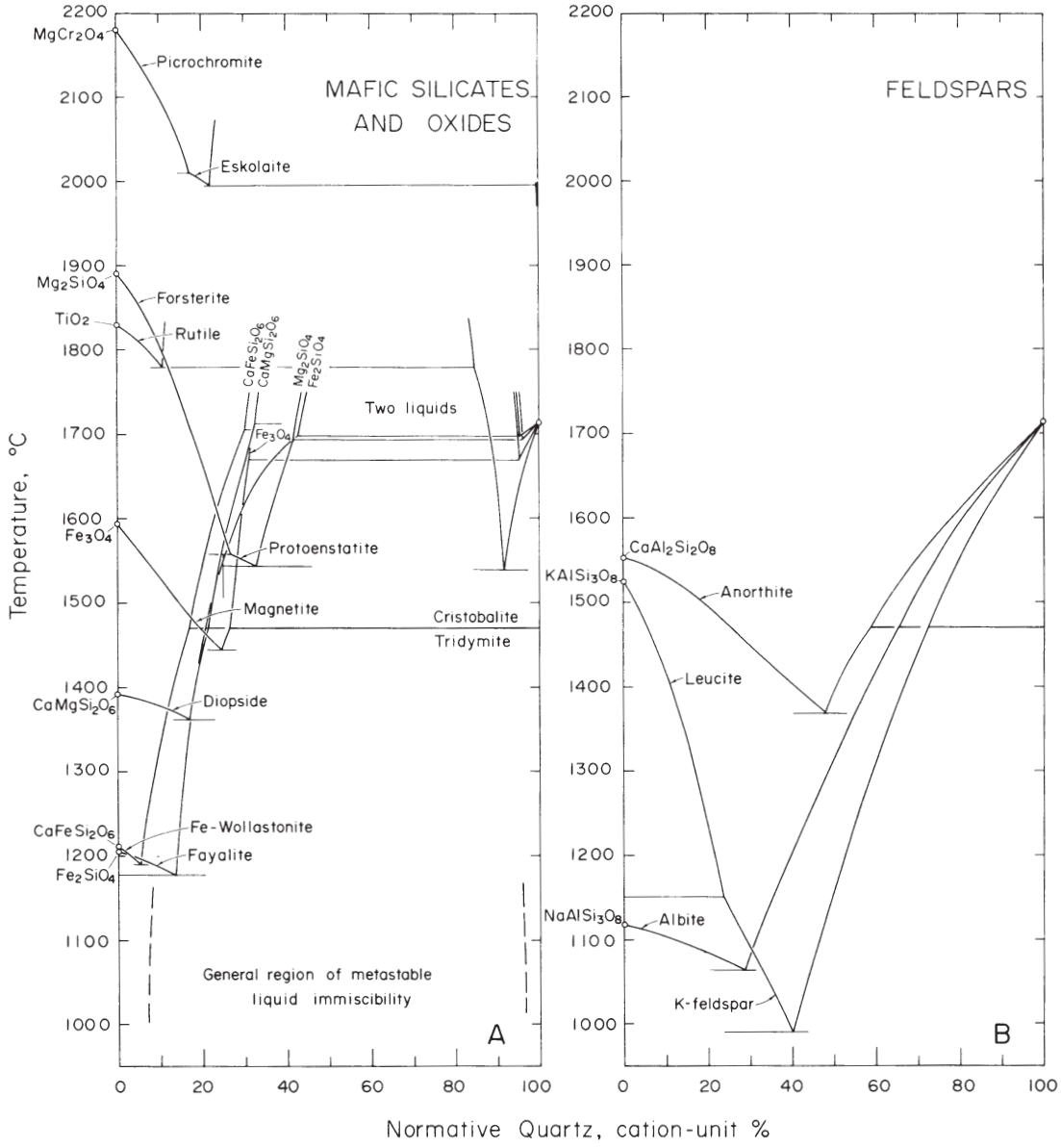

Figure 5. Plot of the 1 atmosphere experimental liquid relations between silica and end-members of the common rock-forming mafic silicates, oxide and feldspar minerals. Note that silica-rich melt shows immiscibility with all mafic minerals and oxide melts but complete miscibility with the feldspar melts, as plotted by Irvine (1975b), using data from Levin et al. (1964; Figs. 80, 82, 113, 266, 412, 508, 586, 599, 715 and 957). [Used by permission of Carnegie Institution of Washington, from Irvine (1975b), *Carnegie Institution of Washington – Yearbook*, Vol. 74, Fig. 57, p. 486.]

Irvine 1975a; see Morse 1980, p. 162), or diopside (Bowen 1914; Kushiro 1972; see Morse 1980, p. 185) to the join Mg_2SiO_4–$MgSiO_3$–SiO_2 slightly extends the MgO–SiO_2 anhydrous binary immiscibility into the ternary systems. The immiscible region then submerges beneath the solidus lowered by the additional component that builds ternary cotectics and eutectics.

The double role of Al_2O_3 in silicate melts

Of greater interest in silicate systems to be applied to natural examples are pseudo-ternary systems where mineral species consisting of two or more oxide components form at least one apex. Very important here are aluminosilicates normally with an alkali element (commonly feldspars and feldspathoids). The role of Al in silicate melts is two-fold, mainly because of its diverse nature (behaving differently in different chemistries and at different pressures). At low pressures, Al mostly forms a four (IV)-coordinated species and joins Si in corner-shared aluminosilicate tetrahedral networks, but it may also act as a network modifier in six (VI)-fold octahedral coordination (at higher pressures).

As is seen in Figure 2c, the Al_2O_3–SiO_2 binary does not show melt immiscibility at lower pressure (1 atm). The solid phases (cristobalite, mullite and corundum), coexisting with silicate liquids, are all very refractory. A metastable solvus has been found at 1 atmosphere beneath the cristobalite liquidus (see MacDowell and Beall 1969; Hudon and Baker 2002a,b). Addition of alkali -or alkaline earth- oxides, causes enormous lowering of liquidus temperatures, eliminates the metastable immiscibility in alumina–silica glasses (MacDowell and Beall 1969) and causes precipitation of feldspars and/or feldspathoids. Hess (e.g., 1995) notes that aluminosilicate units contain tetrahedrally (IV)-coordinated Al^{3+}, which appears to charge-balance mono-or divalent network modifiers. Thus, the molar ratio of Na, K, Ca, (or the typical network modifiers) to Al is an important chemical parameter controlling immiscibility in silicate systems. New spectroscopic work needs to be done to determine the nature and lifetime of certain structural units in the melt (see Farnan and Stebbins 1990; Hans Keppler, personal communication).

Silicate melt immiscibility should be enhanced in "alkaline" compositions (where the sum of the mole-fractions of Na + K + 0.5 Ca + 'network-formers' > the mole fraction of Al) because the excess of network modifiers will tend to form a separate liquid phase (as in the oxide binaries with silica). Conversely, "aluminous" compositions (Na + K + 0.5 Ca + 'network-formers' < Al) will precipitate refractory aluminous crystalline phases from a single homogenous melt, and not show stable immiscibility. The condition where molar Na + K + 0.5 Ca = Al, is special because it defines the compositions of crystalline feldspars and feldspathoids.

Immiscibility in mineral ternary alkali-aluminosilicate melts

Mineral ternary systems thus represent sections through polycomponent composition space relevant to the compositions of magmatic (and metamorphic) rock evolution. Several of such *mineral ternary systems* in *T–X* diagrams show portions with a flat liquidus (like BaO–SiO_2) and thus, presumably hide metastable ternary solvi (e.g., leucite–SiO_2–diopside, nepheline–SiO_2–diopside; as well as albite–fayalite; leucite–forsterite–silica, orthoclase–diopside; Holgate 1954; Barth 1962; Roedder 1978, p. 1611). One particular mineral ternary system (leucite–fayalite–silica) has received a lot of experimental attention because it does indeed show ternary silicate liquid immiscibility (Roedder 1951, 1979). The ternary immiscibility occurs because the lowering of the solidus by the third component is larger than the ternary suppression of the solvus (Barron 1991). The immiscible compositions affect granitic and ferrobasaltic magmatic rocks (enriched in FeO, K_2O and SiO_2) discovered in lunar basalts and in a number of terrestrial igneous rocks (Fig. 6).

Important here are two coincident effects, one is the high FeO-content and the second is the incongruent melting at low pressure of $KAlSi_3O_8$ to leucite ($KAlSi_2O_6$) + SiO_2-rich melt. This permits a re-emergence of the two-liquid immiscibility of the "FeO"–SiO_2 binary into

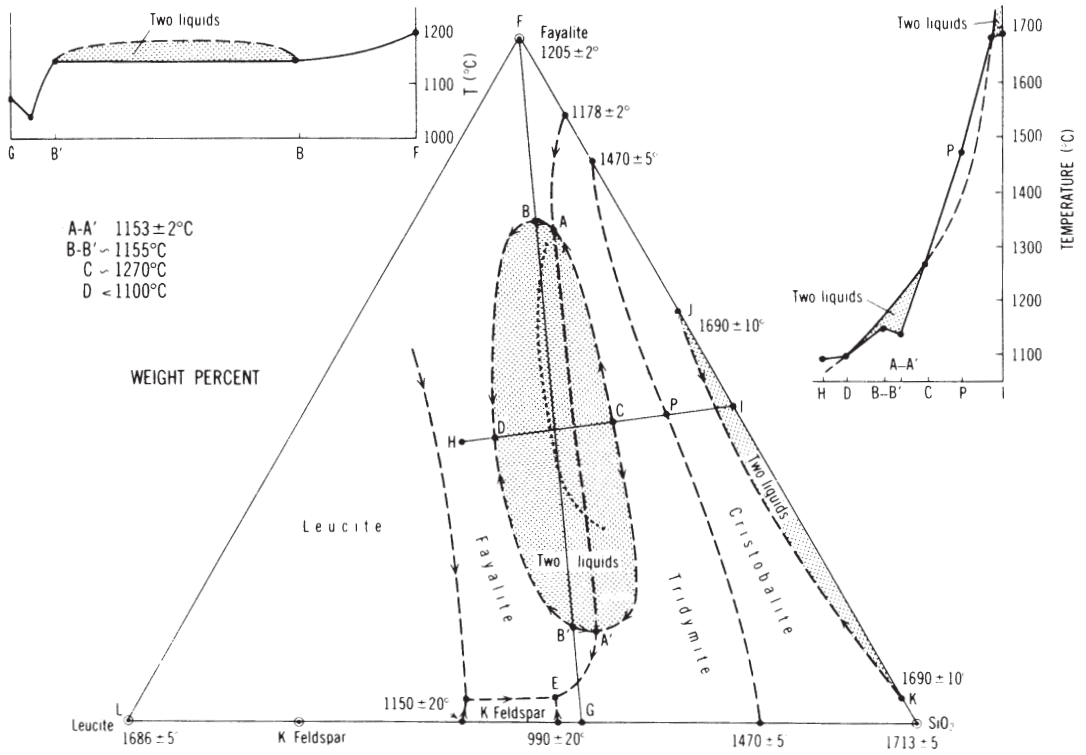

Figure 6. Preliminary diagram of the system leucite–fayalite–SiO_2 (Roedder 1951), showing fields of immiscibility (shaded) at high temperature (along J–K), and at low temperature (A–B–DB′–A′–CA). Dotted line is the 1180 °C isotherm on the upper surface of two-liquid solvus (Watson 1976). The inset figures are *T–X* sections along the lines G-F and H-I. [Used by permission of Elsevier, from Roedder (1978), *Geochimica et Cosmochimica Acta*, Vol. 42, Fig. 2, p. 1601.]

the ternary systems with leucite, along the ternary tridymite + fayalite cotectic. High FeO-contents are significant here because Fe end-members of Fe–Mg silicate solid solutions have low crystallization temperatures (at 1 atmosphere, fayalite (Fe_2SiO_4) melts at 1205 °C, whereas forsterite (Mg_2SiO_4) melts at 1890 °C). Furthermore, pure ferrosilite pyroxene ($FeSiO_3$) is not stable at low pressures, and thus crystallization is suppressed such that polymerized FeO-silica-rich melt develops instead of crystallizing Fe-rich pyroxene. This example demonstrates well the key role of network modifiers (here Fe^{2+}) and the competitive relationships between immiscibility and crystallization (Fig. 6). The analogous Na-system with nepheline ($NaAlSiO_4$)–fayalite–silica (Bowen 1937) does not develop stable ternary immiscibility, partly reflecting compound formation (albite, $NaAlSi_3O_8$) and eutectic behavior between nepheline–albite and albite–SiO_2. The Na- chemical analogue to the feldspathoid leucite ($KAlSi_2O_6$) is the pyroxene mineral jadeite ($NaAlSi_2O_6$), which is not stable at 1 atmosphere pressure with silicate melt.

Tie-lines connecting coexisting immiscible melts run lengthwise along the two-liquid dome in the middle of the fayalite–tridymite field (profile GF in Fig. 6). The SiO_2-rich and the lower-SiO_2 melts could be called felsic and mafic melts respectively. They represent granite and ferrobasalt (fayalite, plagioclase, ilmenite, etc.) immiscibility. Melts arriving by crystallizing tridymite (SiO_2) meet the solvus dome (see inset on top right in Fig. 6, along profile IH) and move either towards fayalite or towards $KAlSi_2O_6$ + SiO_2 depending where they meet relative to point C. They could end their crystallization history at A or A′ respectively, if these points are truly ternary eutectics. Melts beginning on the leucite–fayalite side will meet the dome between B and B′, depending upon initial composition, and end crystallization at D. There is some discussion about the relative temperatures of the possible eutectics A and A′ and the temperature maxima B and B′ along the join GF (e.g., Biggar 1983; Roedder 1983).

There have been several studies of how the other common rock-forming oxide components,

and also pressure, affect the two liquid immiscibility in leucite–fayalite–SiO_2. Replacing some FeO by MgO increases the liquidus temperature and forces the immiscible region below the liquidus (Bogaerts and Schmidt 2006). Nakamura (1974) suggests that the immiscibility gap in leucite–fayalite–SiO_2 is closed at 1.5 GPa. The *supercritical point* describing the transition should be found at some intermediate pressure. Adding small amounts of CaO depresses both the liquidus and the two-melt field, but at higher CaO Hoover and Irvine (1978) noted a re-emergence of immiscibility with ferrobustamite (to about 10 °C above the liquidus). Adding TiO_2 causes a small expansion of the two-melt field (Visser and Koster van Groos 1979b). P_2O_5 expands the two-melt field and depresses the liquidus (Watson 1976; Visser and Koster van Groos 1979a,c; Bogaerts and Schmidt 2006). This occurs despite the fact that no stable immiscibility was reported in the P_2O_5–SiO_2 binary (Levin et al. 1964; Ryerson and Hess 1980). Increased pressure suppresses two-melt immiscibility in the systems just referred to, as in the oxide–SiO_2 binary systems discussed above.

It is likely that terrestrial magmas usually contain H_2O whose effect on immiscibility we have not considered. However, lunar lavas are likely to have been anhydrous. Roedder (1978, p. 1613, his Fig. 8) has plotted the analyses of lunar lavas (obtained with Paul Weiblen) on a more general diagram than leucite–fayalite–SiO_2, i.e. using molar units as (Na_2O+K_2O+Al_2O_3)–(CaO+MgO+FeO+TiO_2+P_2O_5)–SiO_2 in Figure 7.

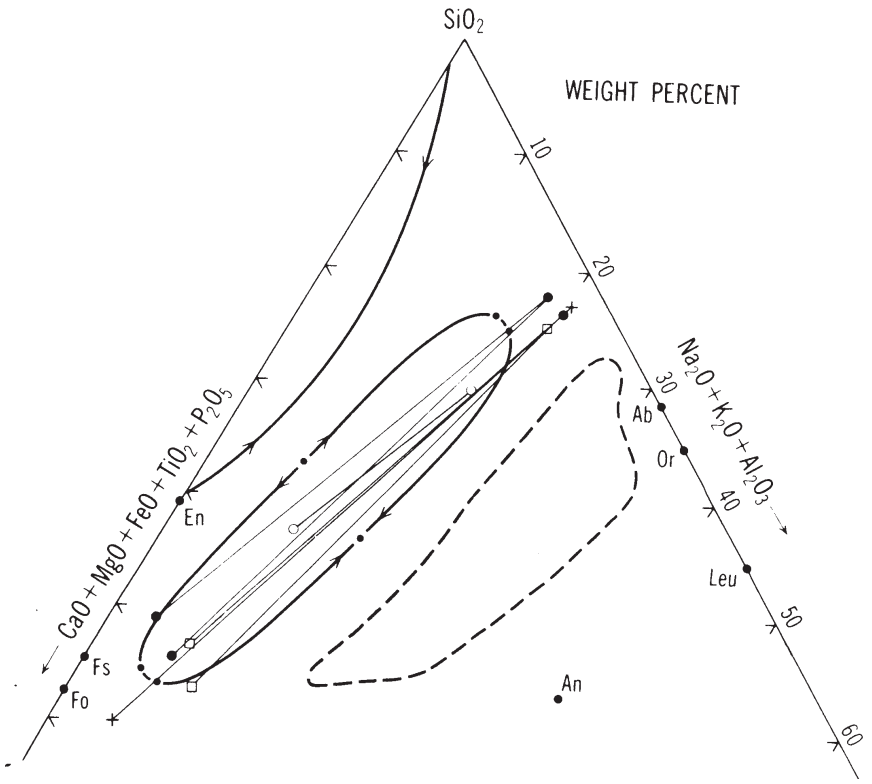

Figure 7. Pseudoternary Greig(*) diagram showing field of low-temperature immiscibility in the system leucite–fayalite–SiO_2. and tie lines for various conjugate melt pairs, adapted from Weiblen and Roedder (1973, 1977). All compositions recalculated on the basis of plotted oxides only: symbols • = coexisting glasses in lunar basalts from Apollo 11, 12 and 15; + = coexisting glasses in lunar basalt 14310; o = synthetic Apollo 11 sample after equilibration at 1045 °C; = Apollo 15 grain. The last item is from Switzer (1975); all other data from Roedder and Weiblen (1970, 1971 and 1972) and Weiblen and Roedder (1973). Other lunar samples are similar but have been omitted for clarity. Most analyzed volcanic rock suites fall within the dashed field (Brooks and Gelinas 1975). (*) <u>*Note*</u> that (Roedder (1979, p.1613) attributes the diagram to Greig (1927b), but Roedder (1978) himself appears to have added TiO_2 and P_2O_5 to the CFM corner. [Used by permission of Elsevier, from Roedder (1978), *Geochimica et Cosmochimica Acta*, Vol. 42, Fig. 8, p. 1613.]

It is quite remarkable that the lunar lavas straddle the two-melt immiscibility dome in the Greig diagram (Fig. 7), a "serendipitous confirmation" of the occurrence of some two-silicate-melt immiscibility in lunar nature. The apparent compositional shift of natural rocks away from silica relative to the field for leucite–fayalite–SiO_2 mainly reflects the unequal effects of the additional components upon immiscibility (e.g., see Holgate 1954).

Summary for anhydrous silicate melt systems

Both increasing pressure and temperature generally decrease silicate immiscibility in anhydrous magmas, so that anhydrous magmas at high temperatures and depth can be of continuous composition from intermediate to siliceous. Distinct chemical effects are also obvious, because increasing CaO and MgO decreases immiscibility, whereas increasing TiO_2 or P_2O_5 promotes immiscibility (Ryerson and Hess 1980; Ryerson 1985; Mysen 1990; Bogaerts and Schmidt 2006). At microscopic scale and with regard to melt structure, the main factors controlling immiscibility phenomena in silicate melts appear to be the Coulombic properties of network-modifying cations (in natural compositions represented mainly by alkalis and alkaline earths) and their relationships to Al (e.g., see Hess 1995: Mysen 2004).

These immiscibility/supercriticality discussions so far have not considered volatile species. The most important magmatic volatile in the Earth is H_2O (e.g., see Hack et al. 2007), but there are important examples where the magmatic volatile is CO_2. Our next section considers anhydrous melts with the addition of CO_2, and with it carbonate melts that sometimes coexist with anhydrous silicate melts.

MOLTEN SILICATE-CARBONATE SYSTEMS

The occurrence of magmatic carbonatites with specific silicate magmatic rocks (alkali basalts, nephelinites, melilitites), and the occurrence of carbonate ocelli in some mantle xenoliths have been suggested as evidence for magmatic silicate–carbonate liquid immiscibility (e.g., Ferguson and Currie 1971; Rankin and Le Bas 1974; Romanchev and Sokolov 1979; Gittins 1989; Bailey 1989, 1993; Barker 1989; Kjarsgaard and Hamilton 1989; Kjarsgaard and Peterson 1991; Church and Jones 1995; Bell 1998). Other occurrences of magmatic carbonate are ascribed to primary carbonate magma from some parts of the mantle, or originate during fractional crystallization of silicate magma (see Bell et al. 1998).

Experimental studies at high pressures, firstly in the system CaO–MgO–SiO_2–CO_2 (= CMS+CO_2, e.g., Wyllie and Huang 1976, Wyllie 1977, and Eggler 1978a,b) addressed the origin of calcic and dolomitic carbonatite magmas and coexisting silicate magmas. Later studies in more complex synthetic systems and natural compositions (e.g., Falloon and Green 1989; Thibault et al. 1992; Dalton and Wood 1993) revealed the extent of the silicate–carbonate miscibility also with sodic carbonatite magmas.

The systematic effects of composition (including Al/Si) and pressure on the silicate carbonate miscibility gaps have been summarized by Lee and Wyllie (1998a,b). Figure 8 shows their reconstruction for phase relations in quite complex silicate–carbonate systems near 1.0 GPa. The 2-liquid field separates silicate liquids from Na-Ca carbonate liquids.

The subsolidus reaction olivine + clinopyroxene + CO_2 = enstatite + dolomite (with forsterite and enstatite in the CMS+CO_2 model system) has a positive dP/dT slope, and produces dolomite when CO_2 is added to mantle rock with increasing depth, and decarbonation (and melting) occurs with increasing temperature. CO_2 replenishment of the mantle wedge is possible by subduction of carbonates. Therefore, beginning at depths > 70 km at a T of ~ 1000 °C, a dolomitic liquid can be produced as a primary melt from carbonated mantle. Figure 9 shows that the solidus curve for a carbonate-bearing peridotite has a sharp kink or ledge at a depth of ~ 70 km (ca. 2 GPa; Wyllie 1978, 1987 1989; Eggler 1978a,b, 1989; Brey et al. 1983; Green and

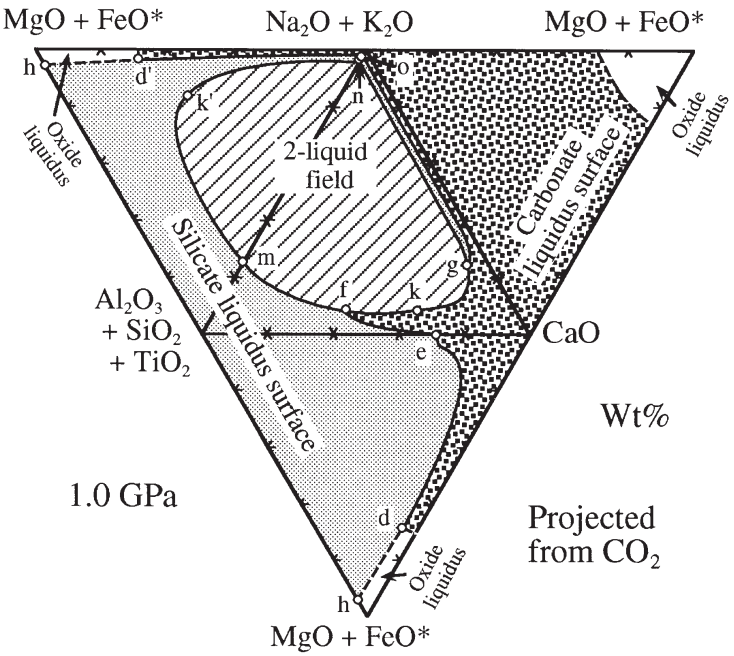

Figure 8 Field boundaries intersected by the end-member triangles of the tetrahedron CaO–(MgO+FeO*)–(Na_2O+K_2O)–(SiO_2+Al_2O_3+TiO_2), projected from CO_2, at 1.0 GPa. Three major fields are defined for the silicate–carbonate liquid miscibility gap (two liquid field), silicate liquidus surface, and carbonate liquidus surface. A small oxide field near the (MgO+FeO*) apex is also sketched. k′ is the critical point for the CaO-free miscibility gap m–k′–n. Point d′ between the carbonate and oxide fields in the CaO-free triangle corresponds to d. [Used by permission of Oxford University Press, from Lee and Wyllie (1998a), *Journal of Petrology*, Vol. 39, Fig. 4, p. 502.]

Wallace 1988; Falloon and Green 1989, 1990) corresponding to the above peridotite + dolomite decarbonation reaction. This ledge is much shallower than that observed experimentally for hydrous mantle, where the ledge for hydrated mantle is at about 95 km (3 GPa, Fig. 9b). Thus the lithosphere-asthenosphere boundary would be interpreted to be able to occur at different depths if the mantle is carbonated (70 km) compared to if the mantle is hydrated (95 km). The "oceanic intraplate" geotherm reintersects the hydrated solidus at a minimum depth of ca. 150 km (base of asthenosphere), hence permitting production of small amounts of a carbonate (still dolomitic and then magnesitic) liquid between 95 and 150 km. A reaction between the dolomitic carbonate liquid and mantle lherzolites produces a calcite carbonate liquid, leaving behind wehrlites (olivine + clinopyroxene) through a reaction simplified as dolomite + orthopyroxene = clinopyroxene + olivine + $2CO_2$ in the complex mantle chemical system. These wehrlites are presumed to act as pipes (conduits) for the calcic-carbonate liquids to pass through on their ascent.

All hypothetical models for the origin of carbonatites invoke the production of a carbonate melt by very small degrees of partial melting reactions involving carbonate minerals in the mantle at rather great depths (200–300 km). Some hypotheses consider primary carbonatite magma, others consider carbonate exsolving as an immiscible liquid phase from or residual to silicate magma during fractionation. At higher pressures (ca. 2.5 GPa) cotectics between carbonate and silicate liquidus surfaces are stable over a considerable range of temperatures. With decreasing pressure, the carbonate and silicate liquidus surfaces retract from one another and become separated due to developing L–L immiscibility (e.g., Fig. 10). So a transition from supercriticality to immiscibility between carbonate and silicate melts occurs during decompression.

Several quite diverse origins have been proposed for carbonatites (e.g., see Bell et al. 1998), some involving immiscibility between carbonate and silicate liquids increasing with decompression. Some carbonatites are proposed as products of crystallization from a primary

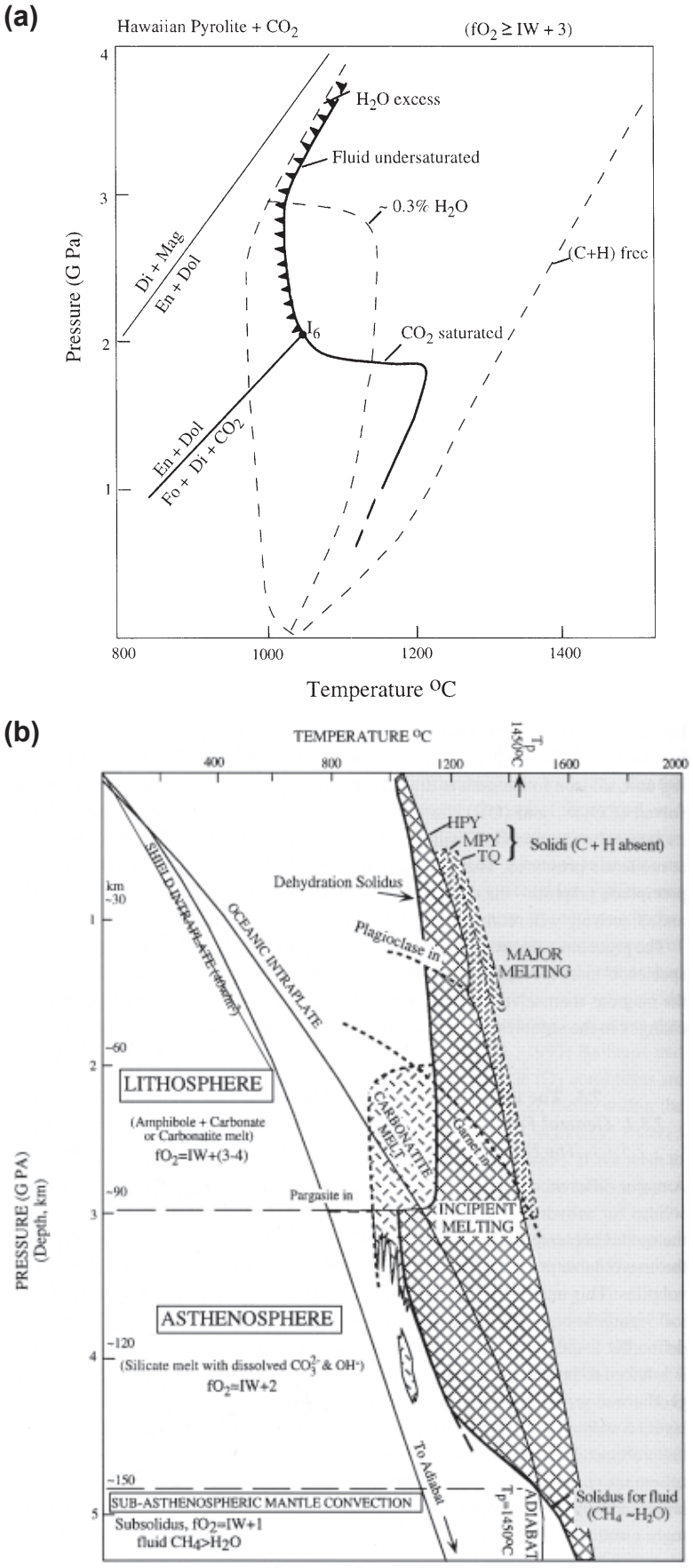

Figure 9. (a) *PT* diagram showing the solidi for Hawaiian pyrolite (a synthetic mixture of 0.25 MORB and 0.75 peridotite) with (C+H+O) compared with the (C+H)-free solidus and the H_2O-saturated and H_2O-undersaturated solidi. These three solidi are shown as short dashed lines. The figure shows the experimentally determined solidus for Hawaiian pyrolite + CO_2 (heavy solid line). The solidus is CO_2-saturated at pressures lower than the intersection of the carbonation reaction with the solidus at I_6 (see Wyllie 1978, 1987). At higher pressures, dolomite is present as a subsolidus phase, the solidus is fluid-undersaturated, and the melt phase is sodic dolomitic carbonatite. (b) The *PT*- experimental data plotted as a function of depth (downwards into the Earth). The oceanic geotherm meets the ledge of the mantle solidus near 95 km, thus defining the base of the lithosphere. The intersection at 150 km defines the base of the asthenosphere in the oceanic mantle. [Used by permission of Cambridge University Press, from Green and Falloon (1998), *The Earth's Mantle – Composition, Structure and Evolution*, Jackson (ed), Chapter 7, Fig. 7.5a, p. 336.]

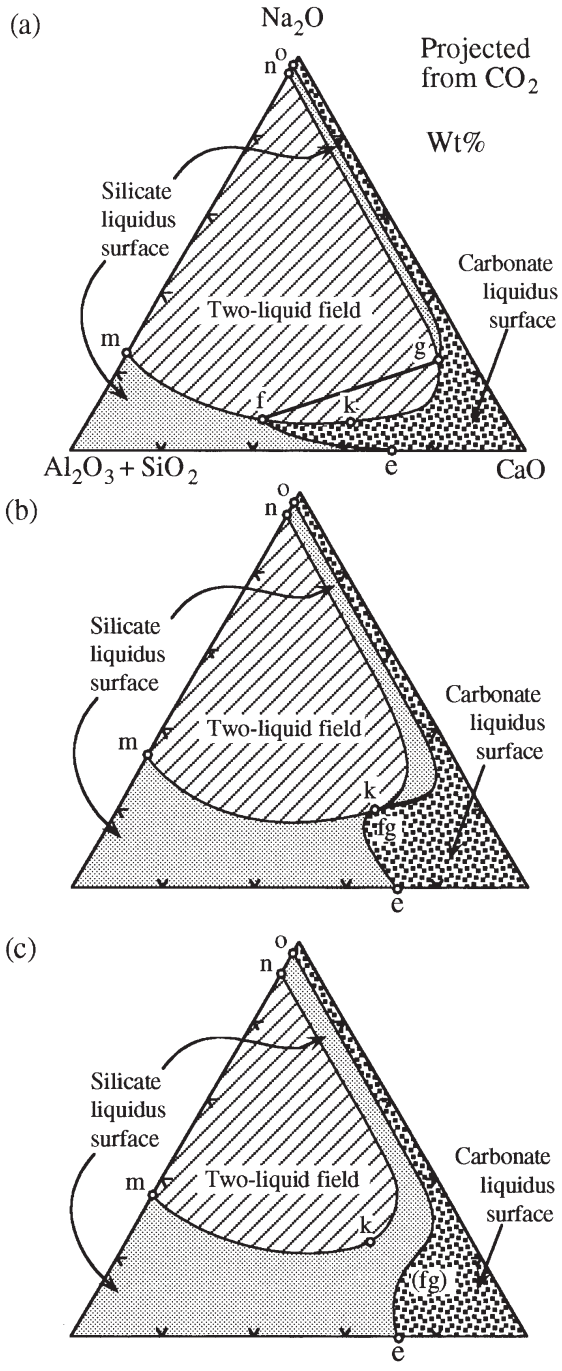

Figure 10. Variation of the geometrical arrangement of silicate–carbonate phase field boundaries as a function of composition. The decrease in size of the miscibility gap (two liquid field) and the nature of the intersection of the two surfaces (silicate, carbonate) occurs from a to b to c, with increasing Al/Si ratio or decreasing pressure; and also decreases with increasing Mg/Ca at constant pressure, (a) The silicate–carbonate liquidus field boundary (e–f, g–n) intersects the miscibility gap field boundary (m–f–k–g–n), at *P* near 1.0 GPa (at 2.5 GPa, point f lies towards point m). (b) The liquidus field boundary is tangential to the miscibility gap field boundary due to increased increasing Al/Si. (c) the two field boundaries are further separated from each other. [Used by permission of Oxford University Press, from Lee and Wyllie (1998a), *Journal of Petrology*, Vol. 39, Fig. 2, p. 449.]

carbonate melt, but experiments have shown that such melts are dolomitic whereas carbonatites are predominantly calcitic in nature). Carbonatite magma produced by these melting reactions and rising through the mantle will solidify at depth prior to reaching the surface, and through cooling release the available volatiles. The association with alkalic rocks reflects widespread fenitization—release of dissolved alkalis and silica from the cooling magma into the surrounding rock, which when of suitable composition reacts with the metasomatising fluids. The shallower… the depth of CO_2 release, the greater the explosion of decarbonation.

Fractional crystallization of an alkalic magma (produced by slightly larger degrees of partial melting in the mantle) does not simply explain why carbonatites are enriched in REE, Zr, Nb, Ta, etc, (although these trace elements could remain incompatible to solids by staying in the liquid during fractionation). If natrocarbonatites are products of liquid immiscibility

from high-Na regions of the mantle, this requires the presence of a significant amount of Na_2CO_3 (at least 5% and up to 20%) in the source region.

Ca-carbonatities and Na-carbonatites show quite different immiscibility behavior (Koster van Groos and Wyllie 1963; Freestone and Hamilton 1980; Kjarsgaard 1998; Lee and Wyllie 1998a; Petibon et al. 1998). The formation of latter being probably more important at low pressures and perhaps related to the fractionation of calcic plagioclase in the silicate magma permitting enrichment of Na in the later carbonatite magma.

Because carbonate liquid is characterized by a very-low viscosity and very-low surface tension (e.g., Rabinowicz et al. 2002), it could be mobilized even at low degrees of partial melting (0.01 vol%).

In sodium-bearing systems (the system Na_2O–CaO–SiO_2–Al_2O_3–CO_2), a silicate melt is immiscible with a Na-carbonate melt, with the result that three phases may coexist: a silicate melt, a Na > Ca carbonate melt and an alkali–rich volatile fluid.

ANHYDROUS MOLTEN SILICATE SYSTEMS WITH PHOSPHOROUS, FLUORINE, CHLORINE, BORON, SULFUR

Additions of even minor amounts of non-silicate anions (sometimes collectively called salts; of phosphorous, fluorine, chlorine, boron, sulfur) appear to have significant effects on liquid immiscibility, also in anhydrous systems. For example, enhancement of liquid immiscibility between silicate melts and liquids of non-silicate anions have been shown in experimental studies on fluorides (Kogarko and Krigman 1970; Gramenitskiy and Shekina 1994; Gramenitskiy et al. 1993; Veksler et al. 1998a,b); chlorides (Webster and DeVivo 2002) and borates (Veksler et al. 2002a,b, 2004, p.17). Experiments indicate that two sulfide liquids, one metal-poor (*M*/S ~1.00) and one metal-rich (*M*/S ~1.14) may exist in parts of the Cu–Ni–Fe–S system (Craig and Kullerud 1969; Kullerud et al. 1969; Cabri 1973). These melts may exist within a crystallized silicate mineral matrix, e.g. sulfides, prominently (Fe, Ni)S solutions, are likely to be molten where present in the upper mantle even at sub-silicate solidus conditions.

Visser and Koster van Groos (1979b) proposed that P_2O_5 strongly increases the miscibility gap between ferrobasaltic and granitic compositions (Fig. 6; Krigman and Krot 1991; Suk 1998). P_2O_5 has a quite different role to the other oxides concerning the modification of silicate melt structure. Ryerson and Hess (1980) noted that P_2O_5 in silicate melts not only produces a marked decrease in silica activity, but co-polymerizes the SiO_2-network rather than modifying the network. In more complex melts with other additional cations (as oxides M_xO_y), *M*–O–P bonds are produced which are stronger than *M*–O–Si bonds. In immiscible granitic+ferrobasaltic melts, P_2O_5 would bond with high charge density cations Fe^{3+}, Mg^{2+}, Mn^{2+}, Mn^{3+}, Ca^{2+}, Cr^{3+} Ti^{4+} in (depolymerized) lower silica melts (Ryerson and Hess 1980). The binaries of these with silica (TiO_2–SiO_2, Fe_2O_3–SiO_2, Cr_2O_3–SiO_2, MnO–SiO_2, Mn_3O_4–SiO_2, etc) have fields of liquid immiscibility at high temperatures that cover almost the whole range of composition (Fig. 2). The El Laco magnetite lava flow in Northern Chile (Park 1961), may owe its formation to phosphorous-enhanced immiscibility and the associated fractionation effects (Sillitoe and Burrows 2002).

Veksler (2004) considers that the general rules and regularities of salt–silicate unmixing and the decisive role of network-modifying cations are the same as in the pure silicate systems, paraphrased: in comparison to the network-modifying cations, the effects of the non-silicate anions on liquid immiscibility are subordinate, indirect and secondary. Their role may be better envisaged as fluxing components which suppress crystallization. They may thus reveal the tendencies for unmixing in silicate melts that are otherwise hidden below liquidus surfaces. Non-silicate anions (P, S, F, Cl, and B) provide a means for network modifiers to separate in the form of salt melts, often with very low-SiO_2 concentrations.

SUPERCRITICAL OR SUPERSOLVUS MELTS IN ANHYDROUS SILICATE ROCK SYSTEMS AT HIGHER PRESSURE?

The available experimental data from binary and ternary systems with silica may be used to explore supercritical phenomena in anhydrous silicate rock systems, relevant to planetary interiors. We have seen that distinct classes of miscibility are found at distinct pressures depending upon the charge and size of the cation in the oxide component with SiO_2. We will examine the available anhydrous melting data to see how miscibility might change with pressure in the Earth, in simplified anhydrous peridotite (model upper mantle), basalt (model oceanic crust) and by comparison for granite (model continental crust).

Simplified peridotite mantle

Anhydrous mantle peridotite can be modeled by olivine + pyroxene. In MgO–FeO–SiO_2 (MFS) that is the olivine+orthopyroxene region. Both the systems MgO–SiO_2 (MS) and FeO–SiO_2 (FS) show regions of two melts at 1 atmosphere (Bowen and Anderson 1914; Bowen and Schairer 1932: summarized in Fig. 2b). The ternary phase diagram MFS contains a two-melt tunnel (Bowen and Schairer 1935), between very SiO_2-rich melt (L_1 in Fig. 4b) and intermediate "basaltic" melt (L_2 in Figure 4b). Two reactions are important; one (at ca. 1695 °C at 1 atm) involving these two melts with one solid, at composition between $MgSiO_3$–SiO_2, which with cooling can be written as the eutectic:

L_1 (SiO_2-rich melt) → L_2 (intermediate melt) + SiO_2-mineral (cristobalite/quartz/coesite)

The other is peritectic and involves two solids, enstatite + forsterite, and one melt (basaltic). The peritectic occurs at lower temperatures (1557 °C) than the eutectic (at ca. 1695 °C, at 1 atm), and can be written with cooling as :

forsterite + L_2 (intermediate "basaltic" melt) → enstatite

It is this second peritectic reaction which generates intermediate "basaltic" melt from lower-SiO_2 compositions by precipitation of forsterite. Melt L_2 finally crystallizes at the eutectic (at 1543 °C):

L_2 ("basaltic" melt) → enstatite + SiO_2-mineral (cristobalite, then quartz)

With increasing pressure in the anhydrous MgO–SiO_2 system, enstatite melting becomes congruent near 0.14 GPa (e.g., Boyd et al. 1964: see Morse 1980, Fig. 18.10, p. 358) so that now forsterite and enstatite are involved in eutectic melting rather than the above-mentioned peritectic. This eutectic (enstatite + forsterite → L_3, Fig. 11d) generates ultramafic liquids upon mantle melting. These ultramafic liquids (L_3, Fig. 11d) have nothing to do with the two-melt liquid immiscibility which involves L_1 and L_2. The two-melt field is confined to the region between the enstatite + cristobalite eutectic and the silica-rich side. Dalton and Presnall (1997) have confirmed that the two-melt field has disappeared below the $MgSiO_3$ + SiO_2 solidus at 5 GPa. They note that the flat liquidus most likely reflects the submerged two-melt solvus (their Fig. 5, p. 2372). According to the data from Hudon et al. (2004), the system MgO–SiO_2 (MS, Fig. 4a) still shows two-melt immiscibility at 1.5 GPa. Our extrapolation (Fig. 4a) for MS shows supercritical intersection between solvus and solidus near 2 GPa. The displacements due to FeO in upper mantle concentrations may lower the critical solvus line and the solidus by similar amounts (lighter lines in Fig. 11a). Thus there is no reason to assume that the equivalent intersection in FeO–SiO_2 (FS) should occur at pressure higher than 2 GPa. This means that melt behavior at high-SiO_2 in anhydrous MFS should also go from immiscible (below ca. 2 GPa) to supercritical at quite shallow mantle depths in the Earth (ca. 75 km). The (*T–x*) diagram in Figure 11d show that at supercritical pressures, a single-melt field is present between $MgSiO_3$ (at B) –SiO_2, and that such anhydrous melts will enter into the two-melt region of coexistence of silicic melt (L_1) with "basaltic" melt (L_2) upon decompression.

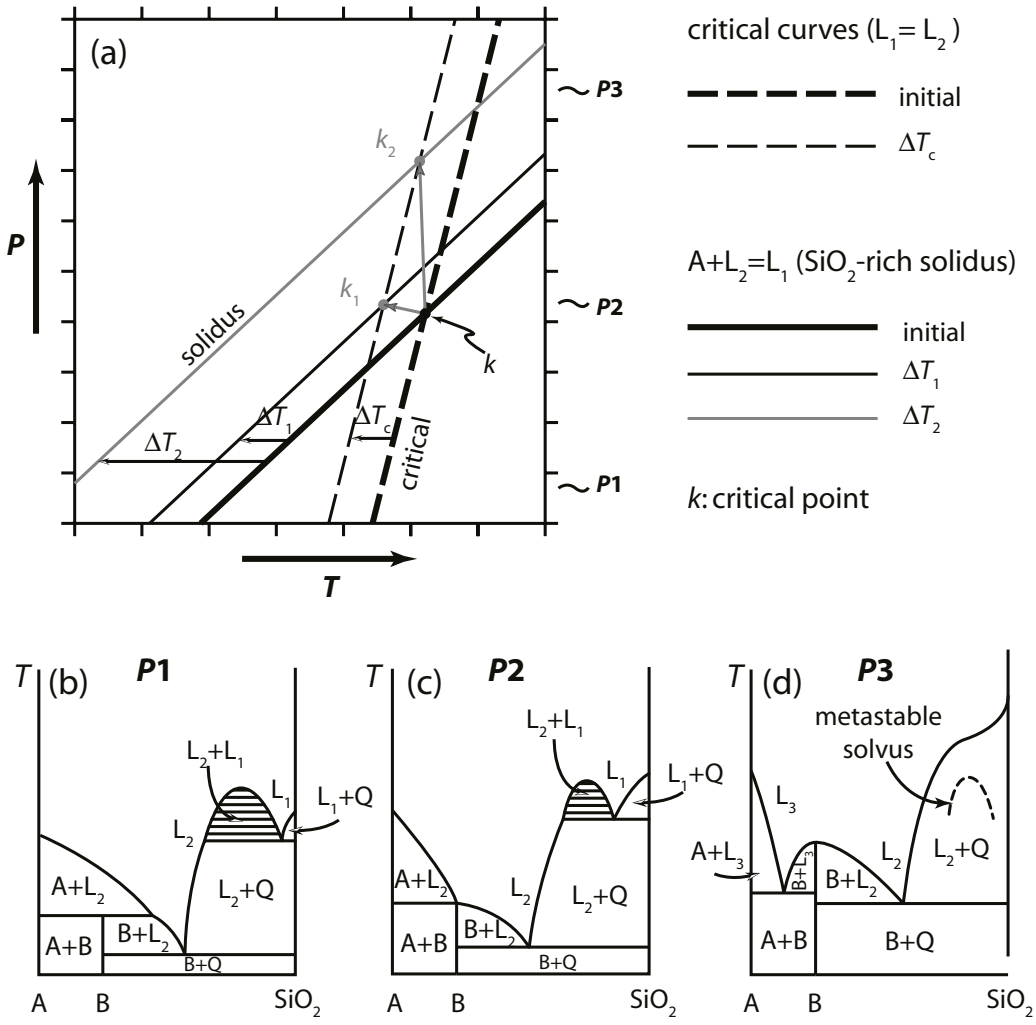

Figure 11. (a) Schematic *PT*-diagram for the anhydrous system A – SiO_2 , showing how further components will influence the location of melting curves (solidi) and solvi, depending on how they partition between solid and melt, relative to the end-member systems illustrated here. Greater solubility will result in a larger ΔT shift ($\Delta T_2 > \Delta T_1$) and thus displacement of the impure critical point *k* to higher pressures at lower temperatures. FeO for example will partition into melt more than mineral (x_{Fe} liquid > x_{Fe} olivine, which is equivalent to x_{Mg} olivine > x_{Mg} liquid; also for pyroxene). The net effect is to displace the solidus to lower *T* more than the solvus (ΔT_1 and ΔT_2 are > than ΔT_C). The net effect is to move the critical point for the end-member system to lower *T* but higher *P* in the impure system. Schematic *T*–*x* sections (b–d) for the anhydrous system A – SiO_2 with intermediate compound B, at $P_3 > P_2 > P_1$. For example in Mg_2SiO_4 (composition A) –SiO_2 for which P_2 = ca. 0.14 GPa, there is a switch from incongruent anhydrous melting of enstatite (composition B, $P_1 < 0.14$ GPa) to congruent ($P_3 > 0.14$ GPa). Q refers to cristobalite as the low-pressure liquidus phase, and quartz as the high-pressure liquidus phase.

While at $P > 2$ GPa all initially siliceous liquids would end up at the "basaltic" eutectic orthopyroxene (enstatite) + SiO_2, this would only be relevant for subducted intermediate and felsic compositions at mantle depths but not for ultramafic mantle rocks.

Simplified basaltic crust

At lower pressure, basalts can be modeled by plagioclase + clinopyroxene + olivine for which there is some approximate data on immiscibility from the appropriate mineral–silica anhydrous binaries (Fig. 5, from Irvine 1975b). The mafic+SiO_2 versus felsic+SiO_2 diagrams of Figure 4 show that basaltic compositions can be modeled by the *P*–*T* relations for supercritical phenomena in olivine with the solidus lowered by plagioclase. We discussed earlier how addition to the join Mg_2SiO_4–$MgSiO_3$–SiO_2 of anorthite (Andersen 1915; Irvine 1975a, see

Morse 1980, p. 162), or diopside (Bowen 1914; Kushiro 1972, see Morse 1980, p. 185) extends the $MgO–SiO_2$ anhydrous binary immiscibility slightly into the ternary systems.

We may consider how additional basaltic components to $MgO–SiO_2$ (Figs. 2b, 4a,b and 11a) might displace the ultramafic (simplified as forsterite + enstatite in MSH) critical phenomena, where with increasing pressure the two melts merge at around 2 GPa, when the solvus and solidus intersect (Fig. 4a). It is the SiO_2-rich melt which becomes miscible with feldspar components to large extent, while the intermediate melt takes in some alkali to become "basaltic".

It is likely that plagioclase and clinopyroxene components added to $MgO–SiO_2$ to make "basalt", may lower the two-melt solvus slightly in temperature, but with much larger *T* lowering of the anhydrous basalt solidus (simplified as cristobalite + enstatite = L_2 in MSH) compared to peridotite (forsterite + enstatite = L_3; Figs. 4, 11).

As shown by the various arrows in Figure 11a, additional components which partition into the melts will displace the $MgO–SiO_2$ ($L_1 = L_2$) critical point to higher pressures but lower temperatures in a basaltic system. This suggested behavior of a higher *P* critical intersection between solvus and solidus, can be seen in the anhydrous $CaMgSi_2O_6–SiO_2$ system in Figure 4c. Basalts are eclogitic at higher pressure. At pressures higher than plagioclase stability, garnet + clinopyroxene show a eutectic (Yoder and Tilley 1962; Pertermann and Hirschmann 2003) so that any solvus lies submerged at lower *T* than the liquidus, i.e. anhydrous eclogite liquids are supersolvus melts.

Simplified felsic crust

Simplified anhydrous granitic compositions can be modeled by anhydrous melting of albite + orthoclase + quartz and considered with reference to the alkali feldspar solvus in "Petrogeny's residua system" (Schairer and Bowen 1955, 1956; Tuttle and Bowen 1958). This name was actually applied by these workers to the water-bearing system with the allusion that all common silicate magmas migrate towards these components following fractional crystallization of higher temperature (and more mafic) minerals.

In the anhydrous system, the alkali feldspar minimum lies at higher temperature than the critical temperature at the top of the solvus, at all pressures. This temperature gap between solvus and solidus introduces supersolvus conditions where the solids are no longer immiscible as they are at lower temperatures.

Thus for the anhydrous system, the alkali feldspars are completely miscible at the solidus. The "minimum" melting for an azeotropic system is supersolvus (called hypersolvus by Tuttle and Bowen 1950) as distinct from supercritical, which occurs following intersection of solvus and solidus (defined in Figs. 4c and 11a). Around 0.4 GPa, the intersection of solidus and solvus (see Tuttle and Bowen 1950; Yoder et al. 1957; Morse 1980 p. 396) allows two feldspars to coexist. The granites are no longer supersolvus, but now eutectic, and we can refer to subcritical melting as that where albite + orthoclase are not completely miscible in the melting assemblage. Hence we are discussing here the relation of critical phenomena (sub-solvus compared to supersolvus) in solidus mineral melting, not melt L–L immiscibility, as in previous examples.

The *P–T* slope of the critical line for the alkali feldspar solvus has been estimated (Waldbaum and JB Thompson 1969). It does intersect the alkali feldspar to jadeite + quartz subsolidus reaction near 2.5 GPa and 1000 °C, but continues to lie at much lower temperatures than the anhydrous granite solidus (e.g., Thompson and Thompson 1976, p. 260). So that at higher pressure anhydrous granite melting is supersolvus with respect to the alkali feldspar minerals but not supercritical, because of lack of intersection of reactions. Felsic compositions buried or subducted to great depths (at least 2 GPa ca. 75 km) at anhydrous melting, will show continuous melt compositions from SiO_2 towards eutectics with feldspathic or intermediate compositions, but no alkali feldspar unmixing (or L–L phenomena).

At low pressures, the alkali feldspar solvus lies some 200 °C lower than the anhydrous solidus. Anhydrous granites are "hypersolvus" (supersolvus). Complete liquid crystallization at low pressures produces a single feldspar at the solidus (albite or orthoclase rich, because of the minimum/eutectic), which upon cooling can exsolve to make (anti-)perthite. Increasing H_2O-pressure lowers the temperature of the solidus enormously with very little increase of the solidus pressure (Tuttle and Bowen 1958).

CONCLUDING REMARKS

Whether oxide–SiO_2 binary systems are immiscible (two coexisting melts) or miscible depends upon size and charge of the other oxide cation. Systems are supercritical when the solidus is at higher *T* than the critical L=L solvus *T*. Supercritical melts have the property that they may coexist with the melting solids up to the liquidus of the system end-members without unmixing. Most 1^+ oxide–SiO_2 systems show submerged solvi, whereas 2^+ oxide–SiO_2 systems show clearly that L–L solvi are stable at higher *T* than solidi. 3^+ oxide–silica and higher (4^+, 5^+) oxide–silica systems (Fig. 2) show often the formation of intermediate compounds with high melting points which divide up the oxide–silica join, but still submerged L–L solvi are sometimes found at the high-SiO_2 end.

Binary immiscibility disappears in most ternary, and more component systems, with the exception of Fe_2SiO_4–$KAlSi_2O_6$–SiO_2. Here the lowering of the solidus by the FeO-component relative to the K_2O-component is greater than the *T*-lowering of the L–L solvus. This causes a reemergence of the binary two-melt field in the middle of the ternary system. Further oxide components added to fayalite–leucite–silica diminish the two-melt immiscibility.

Increased pressure in anhydrous silicate systems has the general tendency to cause intersection of solidi and L–L solvi, so that immiscible systems at low pressure become supercritical at higher pressures.

The systematic *P–T* displacement effects of additional components can be predicted for anhydrous natural compositions. Anhydrous magma systems during cooling and fractionation override the intermediate immiscibility of low-pressure binary systems, with the effect that only in the late stages of anhydrous magma fractionation liquid–liquid immiscibility involving silicate-only components is likely to be common. At higher pressures supercritical melt phenomena may also be found in multi-component magma systems at mantle depths, but the very-high temperatures required are probably not found in the current Earth.

Other volatile components (S, C, F, P, Cl, H_2O) can induce and extend immiscibility from anhydrous silicate systems. These components may well be responsible for some documented examples of immiscibility in terrestrial as well as lunar lavas.

The terminology and examples of supercritical behavior has become much more developed in volatile systems than in anhydrous silicate systems. The essential terrestrial ingredient – water, is involved in many inorganic natural systems including silicate melts in magmas, and in the fluids/vapors they evolve upon cooling. This is witnessed by most of the papers in this volume.

ACKNOWLEDGMENTS

ABT wishes to acknowledge Ed Roedder and JB Thompson for discussions over several years. We thank Michael Bogaerts, Peter Ulmer and Max Schmidt for their discussions on immiscibility and supercriticality, Ursula Stidwill for help with the text, and Hans Keppler and Axel Liebscher for their reviews and suggestions.

This work was supported by the Swiss National Science Foundation.

REFERENCES

Alekseeva ZD (1963) Phase diagram of the system Rb_2SiO_3-SiO_2. Russ J Inorg Chem 8:1426-1430 (in Russian)

Andersen O (1915) The system anorthite-forsterite-silica. Am J Sci 39:407-454

Aramaki S, Roy R (1962) Revised phase diagram for the system Al_2O_3-SiO_2. J Am Ceram Soc 45:229-242

Bailey DK (1989) Carbonate melt from the mantle in the volcanos of southeast Zambia. Nature 338:415-418

Bailey DK (1993) Carbonate magmas. J Geol Soc London 150:637-651

Ball RGJ, Mignanelli MA, Barry TI, Gisby JA (1993) The calculation of phase-equilibria of oxide core concrete systems. J Nucl Mater 201:238-249

Baret G, Madar R, Bernard C (1991) Silica-based oxide systems. 1. Experimental and calculated phase-equilibria in silicon, boron, phosphorus, germanium, and arsenic oxide mixtures. J Electrochem Soc 138:2830-2835

Barker DS (1989) Field relations of carbonatites. *In*: Carbonatites: Genesis and Evolution. Bell K (ed) Unwin Hyman, p 38-69

Barron LM (1991) A possible solvus geometry for liquation in quartz-fayalite-leucite. Geochim Cosmochim Acta 55: 761-767

Barth TFW (1962) Theoretical Petrology, 2nd edition. John Wiley

Bedard JH (1994) Mesozoic east North American alkaline magmatism.1. Evolution of Monteregian lamprophyres, Quebec, Canada. Geochim Cosmochim Acta 58:95-112

Bell K (1998) Radiogenic isotope constraints on relationships between carbonatites and associated silicate rocks - a brief review. J Petrol 39:1987-1996

Bell K, Kjarsgaard BA, Simonetti A (1998) Carbonatites - into the twenty-first century. J Petrol 39:1839-1845

Biggar GM (1979) Immiscibility in tholeiites. Mineral Mag 43:543-544

Biggar GM (1983) A reassessment of phase-equilibria involving 2 liquids in the system K_2O-Al_2O_3-FeO-SiO_2. Contrib Mineral Petrol 82:274-283

Bogaerts M, Schmidt MW (2006) Experiments on silicate melt immiscibility in the system Fe_2SiO_4-$KAlSi_3O_8$-SiO_2-CaO-MgO-TiO_2-P_2O_5 and implications for natural magmas. Contrib Mineral Petrol 152:257-274

Bowen NL (1914) The ternary system: diopside – forsterite – silica. Am J Sci 38:207-264

Bowen NL (1928) The Evolution of the Igneous Rocks. Dover Publications Inc.

Bowen NL (1937) Recent high-temperature research on silicates and its significance in igneous geology. Am J Sci 33:1-21

Bowen NL, Andersen O (1914) The binary system MgO-SiO_2. Am J Sci 37:487-500

Bowen NL, Schairer JF (1932) The system FeO-SiO_2. Am J Sci 24:177-213

Bowen NL, Schairer JF (1935) The system MgO-FeO-SiO_2. Am J Sci 29:151-217

Boyd FR, England JL (1960) Apparatus for phase-equilibrium measurements at pressures up to 50 kilobars and temperatures up to 1750 °C. J Geophys Res 65:741-748

Boyd FR, England JL (1963) Effect of pressure on the melting of diopside, $CaMgSi_2O_6$, and albite, $NaAlSi_3O_8$, in the range up to 50 kilobars. J Geophys Res 68:311-323

Boyd FR, England JL, Davis BTC (1964) Effects of pressure on the melting and polymorphism of enstatite, $MgSiO_3$. J Geophys Res 69:2101-2109

Brey G, Brice WR, Ellis DJ, Green DH, Harris KL, Ryabchikov ID (1983) Pyroxene-carbonate reactions in the upper mantle. Earth Planet Sci Lett 62:63-74

Bridgman PW (1927) The breakdown of atoms at high pressure. Phys Rev 29:0188-0191

Brooks C, Gelinas L (1975) Immiscibility and ancient and modern volcanism. Carnegie Institution of Washington Yearbook 74:240-247

Budnikov PP, Cherepanov AM (1953) Lithium-silicate compounds. Russ Chem Rev 22:821-837 (in Russian)

Bunting EN (1930a) Phase equilibria in the system SiO_2-ZnO. J Am Ceram Soc 13:5-10

Bunting EN (1930b) Phase equilibria in the system Cr_2O_3-SiO_2. J Res Nat Bur Stand 5:325-327

Bunting EN (1930c) Phase-equilibria in the system SiO_2-ZnO. J Res Nat Bur Stand 4:131-136

Butterman WC, Foster WR (1967) Zircon stability and ZrO_2-SiO_2 phase diagram. Am Mineral 52:880-885

Cabri LJ (1973) New data on phase relations in the Cu-Fe-S system. Econ Geol 68:443-454

Charles RJ (1966) Metastable liquid immiscibility in alkali metal oxide-silica systems. J Am Ceram Soc 49:55-62

Chen CH, Presnall DC (1975) The system Mg_2SiO_4-SiO_2 at pressures up to 25 kbar. Am Mineral 60:398-406

Church AA, Jones AP (1995) Silicate-carbonate immiscibility at Oldoinyo-Lengai. J Petrol 36:869-889

Circone S, Agee CB (1995) Effect of pressure on cation partitioning between immiscible liquids in the system TiO_2-SiO_2. Geochim Cosmochim Acta 59:895-907

Craig JR, Kullerud G (1969) Phase relations in the Cu-Fe-Ni-S system and their application to magmatic ore deposits. *In*: Magmatic Ore Deposits. Vol 4. Wilson HDB (ed) Economic Geology Publ., p 344-358

Dalton JA, Presnall DC (1997) No liquid immiscibility in the system $MgSiO_3$-SiO_2 at 5.0 GPa. Geochim Cosmochim Acta 61:2367-2373

Dalton JA, Wood BJ (1993) The compositions of primary carbonate melts and their evolution through wallrock reaction in the mantle. Earth Planet Sci Lett 119:511-525
Davis RF, Pask JA (1972) Diffusion and reaction studies in system Al_2O_3-SiO_2. J Am Ceram Soc 55:525-531
DeVries RC, Roy R, Osborn EF (1954) The system TiO_2-SiO_2. Brit Ceram Trans J 53:525-540
Dixon S, Rutherford MJ (1979) Plagiogranites as late-stage immiscible liquids in ophiolite and mid-ocean ridge suites : an experimental study. Earth Planet Sci Lett 45:45-60
Eggler DH (1978a) Effect of CO_2 upon partial melting of peridotite in system Na_2O-CaO-Al_2O_3-MgO-SiO_2-CO_2 to 35 Kb, with an analysis of melting in a peridotite-H_2O-CO_2 system. Am J Sci 278:305-343
Eggler DH (1978b) Stability of dolomite in a hydrous mantle, with implications for mantle solidus. Geology 6:397-400
Eggler DH (1989) Carbonatites, primary melts, and mantle dynamics. *In*: Carbonatites: Genesis and Evolution. Bell K (ed) Unwin Hyman, p 561-579
Falloon TJ, Green DH (1989) The solidus of carbonated, fertile peridotite. Earth Planet Sci Lett 94:364-370
Falloon TJ, Green DH (1990) Solidus of carbonated fertile peridotite under fluid-saturated conditions. Geology 18:195-199
Farnan I, Stebbins JF (1990) High-temperature ^{29}Si NMR investigation of solid and molten silicates. J Am Chem Soc 112:32-39
Ferguson J, Currie KL (1971) Evidence of liquid immiscibility in alkaline ultrabasic dikes at Callander Bay, Ontario. J Petrol 12:561-586
Fields JM, Dear PS, Brown JJ (1972) Phase equilibria in the system BaO-SrO-SiO_2. J Am Ceram Soc 55:585-588
Foley SF (1984) Liquid immiscibility and melt segregation in alkaline lamprophyres from Labrador. Lithos 17:127-137
Freestone IC (1978) Liquid immiscibility in alkali-rich magma. Chem Geol 23:115-123
Freestone IC, Hamilton DL (1980) The role of liquid immiscibility in the genesis of carbonatites: an experimental study. Contrib Mineral Petrol 73:105-117
Ghanbari-Ahari K, Brett NH (1988a) Phase-equilibria and microstructure in the system ZrO_2-MgO-SiO_2-SrO: 1. The ternary Systems ZrO_2-SiO_2-SrO and ZrO_2-MgO-SrO. Calphad 87:27-32
Ghanbari-Ahari K, Brett NH (1988b) Phase-equilibria and microstructure in the system ZrO_2-MgO-SiO_2-SrO: 2. The ternary system MgO-SiO_2-SrO. Calphad 87:103-106
Gittins J (1989) The origin and evolution of carbonatite magmas. *In*: Carbonatites: Genesis and Evolution. Bell K (ed) Unwin Hyman, , p 580-599
Glasser FP (1958) The system MnO-SiO_2. Am J Sci 256:398-412
Gramenitskiy YN, Shekina TI (1994) Phase relationships in the liquidus part of a granitic system containing fluorine. Geochem Int 31:52–70
Gramenitskiy YN, Shekina TI, Berman DP, Popenko DP (1993) Lithium concentration by aluminofluoride melt in a granitic system containing fluorine. Trans Russian Acad Sci 331A:139-144
Green DH, Falloon TJ (1998) Pyrolite: a ringwood concept and its current expression. *In*: The Earth's Mantle: Structure, Composition and Evolution. Jackson I (ed) Cambridge University Press, p 311-378
Green DH, Wallace ME (1988) Mantle metasomatism by ephemeral carbonatite melts. Nature 336:459-462
Greig JW (1927a) Immiscibility in silicate melts, part 1. Am J Sci 13:133-154
Greig JW (1927b) Immiscibility in silicate melts, part 2. Am J Sci 13:1-44
Hack AC, Thompson AB, Aerts M (2007) Phase relations involving hydrous silicate melts, aqueous fluids, and minerals. Rev Mineral Geochem 65:129-185
Hageman VBM, Oonk HAJ (1986) Liquid immiscibility in the SiO_2 + MgO, SiO_2 + SrO, SiO_2 + La_2O_3, and SiO_2 + Y_2O_3 systems. Phys Chem Glasses 27:194-198
Hageman VBM, Van den Berg GJK, Janssen HJ, Oonk HAJ (1986) A reinvestigation of liquid immiscibility in the SiO_2-CaO system. Phys Chem Glasses 27:100-106
Haller W, Blackburn DH, Simmons J (1974) Miscibility gaps in alkali-silicate binaries – data and thermodynamic interpretation. National Bureau of Standards, Washington DC 20234:120-126
Hazen RM, Downs RT (eds) (2001) High-Temperature and High-Pressure Crystal Chemistry. Reviews in Mineralogy and Geochemistry. Vol 41. Mineralogical Society of America
Hemley RJ (ed) (1999) Ultrahigh-Pressure Mineralogy: Physics and Chemistry of the Earth's Deep Interior. Reviews in Mineralogy. Vol 37. Mineralogical Society of America
Hess PC (1980) Polymerization model for silicate melts. *In*: Physics of Magmatic Processes. Hargraves RB (ed) Princeton Press, p 3-48
Hess PC (1995) Thermodynamic mixing properties and the structure of silicate melts. Rev Mineral 32:145-190
Hess PC (1996) Upper and lower critical points: Thermodynamic constraints on the solution properties of silicate melts. Geochim Cosmochim Acta 60:2365-2377
Holgate NJ (1954) The role of liquid immiscibility in igneous petrogenesis. J Geology 62:439-480
Hoover JD, Irvine TN (1978) System Mg_2SiO_4-Fe_2SiO_4-$CaMgSi_2O_6$-$CaFeSi_2O_6$-$KAlSi_3O_8$-SiO_2 and its bearing on silica enrichment trends. Trans-Am Geophys Union 59:1217-1217

Hudon P, Baker DR (2002a) The nature of phase separation in binary oxide melts and glasses. I. Silicate systems. J Non-Cryst Solids 303:299-345

Hudon P, Baker DR (2002b) The nature of phase separation in binary oxide melts and glasses. II. Selective solution mechanism. J Non-Cryst Solids 303:346-353

Hudon P, Jung IH, Baker DR (2004) Effect of pressure on liquid-liquid miscibility gaps: A case study of the systems CaO-SiO_2, MgO-SiO_2, and $CaMgSi_2O_6$-SiO_2. J Geophys Res-Sol Ea 109:B03207

Huntelaar ME, Cordfunke EHP, Scheele A (1993) Phase relations in the SrO-SiO_2-ZrO_2 System: 1. The System SrO-SiO_2. J Alloys Compd 191:87-90

Irvine TN (1975a) Olivine-pyroxene-plagioclase relations in the system Mg_2SiO_4-$CaAl_2Si_2O_8$-$KAlSi_3O_8$-SiO_2 and their bearing on the differentiation of stratiform intrusions. Carnegie I Wash 74:492-500

Irvine TN (1975b) The silica immiscibility effect in magmas. Carnegie I Wash 74:484-492

Jakobsen JK, Veksler IV, Tegner C, Brooks CK (2005) Immiscible iron- and silica-rich melts in basalt petrogenesis documented in the Skaergaard intrusion. Geology 33:885-888

Jung I (2003) Critical evaluation and thermodynamic modeling of phase equilibria in multicomponent oxide systems. Ph.D. thesis, Ecole Polytech. de Montreal, Canada

Kaufman L (1988) System TiO_2-SiO_2. Physica B & C 150:99-114

Kawamoto Y, Tomozawa M (1981) Prediction of immiscibility boundaries of the systems K_2O-SiO_2, K_2O-Li_2O-SiO_2, K_2O-Na_2O-SiO_2, and K_2O-BaO-SiO_2. J Am Ceram Soc 64:289-292

Kim SS, Sanders TH (1991) Thermodynamic modeling of phase diagrams in binary alkali silicate systems. J Am Ceram Soc 74:1833-1840

Kjarsgaard BA (1998) Phase relations of a carbonated high-CaO nephelinite at 0.2 and 0.5 GPa. J Petrol 39:2061-2075

Kjarsgaard BA, Hamilton DL (1989) The genesis of carbonatites by liquid immiscibility. *In*: Carbonatites: Genesis and Evolution. Bell K (ed) Unwin Hyman, p 388-404

Kjarsgaard BA, Peterson T (1991) Nephelinite-carbonatite liquid immiscibility at Shombole Volcano, East-Africa - petrographic and experimental evidence. Mineral Petrol 43:293-314

Kogarko LN, Krigman LD (1970) Phase equilibria in system nepheline-NaF. Geochem Int 7:103-107

Koster van Groos AF, Wyllie PJ (1963) Experimental data bearing on role of liquid immiscibility in genesis of carbonatites. Nature 199:801-802

Kracek FC (1930) The cristobalite liquidus in the alkali oxide-silica systems and the heat of fusion of cristobalite. J Am Chem Soc 52:1436-1442

Kracek FC (1932) The ternary system, K_2SiO_3-Na_2SiO_3-SiO_2. J Phys Chem 36:2529-2542

Krigman LD, Krot TV (1991) Stable phosphate aluminosilicate liquation in magmatic melts. Geokhimiya 11:1548–1560 (in Russian)

Kullerud G, Yund RA, Moh GH (1969) Phase relations in the Cu-Fe-S, Cu-Ni-S, and Fe-Ni-S systems. *In*: Magmatic Ore Deposits. Vol 4. Wilson HDB (ed) Economic Geology Publ., p 323-343

Kushiro I (1972) Determination of liquidus relations in synthetic silicate systems with electron microprobe analysis: the system forsterite-diopside-silica at 1 atmosphere. Am Mineral 57:1260-1271

Lee WJ, Wyllie PJ (1998a) Petrogenesis of carbonatite magmas from mantle to crust, constrained by the system CaO-(MgO+FeO*)-(Na_2O+K_2O)-(SiO_2+Al_2O_3+TiO_2)-CO_2. J Petrol 39:495-517

Lee WJ, Wyllie PJ (1998b) Processes of crustal carbonatite formation by liquid immiscibility and differentiation, elucidated by model systems. J Petrol 39:2005-2013

Levelt Sengers JMH (2000) Supercritical Fluids: Their properties and applications. *In*: Supercritical Fluids. Vol 366. Kiran E, Debenedetti PG, Peters CJ (eds) NATO Science Series E Applied Sciences, p 1-30

Levin EM, Robbins CR, McMurdie HF (1964) Phase Equilibria Diagrams. American Ceramic Society

Longhi J (1990) Silicate liquid immiscibility in isothermal crystallization experiments. Proc Lunar Planet Sci Conf 20:13-24

MacDowell JF, Beall GH (1969) Immiscibility and crystallization in Al_2O_3-SiO_2 glasses. J Am Ceram Soc 52:17-25

Michels MAJ, Wesker E (1988) A network model for the thermodynamics of multicomponent silicate melts: 1. Binary mixtures MO-SiO_2. Calphad 12:111-126

Morgan RA, Hummel FA (1949) Reactions of BeO and SiO_2 - synthesis and decomposition of phenacite. J Am Ceram Soc 32:250-255

Moriya Y, Warrington DH, Douglas RW (1967) A study of metastable liquid-liquid immiscibility in some binary and ternary alkali silicate glasses. Phys Chem Glasses 8:19-25

Morse SA (1980) Basalts and Phase Diagrams. Springer-Verlag

Mysen BO (1990) Relationships between silicate melt structure and petrologic processes. Earth-Sci Rev 27:281-365

Mysen BO (2004) Element partitioning between minerals and melt, melt composition and melt structure. Chem Geol 213:1-16

Nakamura Y (1974) The system SiO_2-H_2O-H_2 at 15 kbar. Carnegie I Wash 73:259-263

Ol'shanskii YI (1951) Equilibrium of two immiscible liquids in silicate systems of alkali-earth metals. Dokl Akad Nauk SSSR 76:93-96 (in Russian)
Park CF (1961) A magnetite "flow" in northern Chile. Econ Geol 56:431-436
Pertermann M, Hirschmann MM (2003) Anhydrous partial melting experiments on MORB-like eclogite: Phase relations, phase compositions and mineral-melt partitioning of major elements at 2-3 GPa. J Petrol 44:2173-2201
Petibon CM, Kjarsgaard BA, Jenner GA, Jackson SE (1998) Phase relationships of a silicate-bearing natrocarbonatite from Oldoinyo Lengai at 20 and 100 MPa. J Petrol 39:2137-2151
Phillips B, Muan A (1959) Phase equilibria in the system CaO-iron oxide-SiO_2 in air. J Am Ceram Soc 42:413-423
Philpotts AR (1976) Silicate liquid immiscibility: its probable extent and petrogenetic significance. Am J Sci 276:1147-1177
Philpotts AR (1982) Compositions of immiscible liquids in volcanic rocks. Contrib Mineral Petrol 80:201-218
Philpotts AR, Doyle CD (1983) Effect of magma oxidation-state on the extent of silicate liquid immiscibility in a tholeiitic basalt. Am J Sci 283:967-986
Prigogine I, Defay R (1954) Chemical Thermodynamics. Longmans
Rabinowicz M, Ricard Y, Gregoire M (2002) Compaction in a mantle with a very small melt concentration: Implications for the generation of carbonatitic and carbonate-bearing high alkaline mafic melt impregnations. Earth Planet Sci Lett 203:205-220
Rankin AH, Le Bas MJ (1974) Liquid immiscibility between silicate and carbonate melts in naturally occurring ijolite magma. Nature 250:206-209
Roedder E (1951) Low temperature liquid immiscibility in the system K_2O-FeO-Al_2O_3-SiO_2. Am Mineral 36:282-286
Roedder E (1978) Silicate liquid immiscibility in magmas and in system K_2O-FeO-Al_2O_3-SiO_2 - example of serendipity. Geochim Cosmochim Acta 42:1597-1617
Roedder E (1979) Silicate Liquid Immiscibility in Magmas. *In*: The Evolution of the Igneous Rocks, Fiftieth Anniversary Perspectives. Yoder HSJ (ed) Princeton University Press, p 15-57
Roedder E (1983) Discussion of "A re-assessment of phase equilibria involving two liquids in the system K_2O-Al_2O_3-FeO-SiO_2", by G.M. Biggar. Contrib Mineral Petrol 82:284-290
Roedder E, Weiblen PW (1970) Lunar petrology of silicate melt inclusions. Apollo 11 rocks. Proc Apollo 11 Lunar Sci Conf, Geochim Cosmochim Acta Suppl 1 1:801-837
Roedder E, Weiblen PW (1971). Petrology of silicate melt inclusions, Apollo 11 and Apollo 12 and terrestrial equivalents. Proc Second Lunar Sci Conf, Geochim Cosmochim Acta Suppl. 2 1:507-528
Roedder E, Weiblen PW (1972). Petrographic features and petrologic significance of melt inclusions in Apollo 14 and I5 rocks. Proc Third Lunar Sci Conf, Geochim Cosmochim Acta Suppl 3 1:251-279
Roedder E, Weiblen PW (1977). Compositional variation in late-stage differentiates in mare lavas, as indicated by silicate melt inclusions. Proc Eighth Lunar Sci Conf, Geochim Cosmochim Acta Suppl. 8 2:1767-1783
Romanchev BP, Sokolov SV (1979) Liquation in the production and geochemistry of the rocks in carbonatite complexes. Geochem Int 16:125-135
Rosenbusch H (1872) Mikroskopische Physiographie der Mineralien und Gesteine. Schweizerbartsche Verlagsbuchhandlung
Ryerson FJ (1985) Oxide solution mechanisms in silicate melts: systematic variations in the activity coefficient of SiO_2. Geochim Cosmochim Acta 49:637-649
Ryerson FJ, Hess PC (1978) Implications of liquid-liquid distribution coefficients to mineral-liquid partitioning. Geochim Cosmochim Acta 42:921-932
Ryerson FJ, Hess PC (1980) The role of P_2O_5 in silicate melts. Geochim Cosmochim Acta 44:611-624
Samsonov GV (1982) The Oxide Handbook, 2nd ed. IFI/Plenum Publishing, New York
Schairer JF, Bowen NL (1955) The system K_2O-Al_2O_3-SiO_2. Am J Sci 253:681-746
Schairer JF, Bowen NL (1956) The system Na_2O-Al_2O_3-SiO_2. Am J Sci 254:129-195
Seward TP, Uhlmann DR, Turnbull D (1968a) Phase separation in system BaO-SiO_2. J Am Ceram Soc 51:278-285
Seward TP, Uhlmann DR, Turnbull D (1968b) Development of 2-phase structure in glasses with special reference to system BaO-SiO_2. J Am Ceram Soc 51:634-643
Shannon RD (1976) Revised effective ionic radii and systematic studies of interatomic distances in halides and chalcogenides. Acta Crystallogr A32:751–767
Sillitoe RH, Burrows DR (2002) New field evidence bearing on the origin of the El Laco magnetic deposit, Northern Chile. Econ Geol 97:1101-1109
Singleton EL, Carpenter L, Lundquist RV (1962) Studies of the MnO-SiO_2 binary system. U.S. Bureau of Mines - Report Investigation 5938:1-31
Stanley E (1971) Introduction to phase transitions and critical phenomena. Oxford University Press

Staronka A, Pham H, Rolin M (1968) Étude du système silice-alumine par la méthode des courbes de refroidissement. Rev Int Haut Temp Refract 5:111-115

Stebbins JF, McMillan PR, Dingwell DB (eds) (1995) Structure, Dynamics and Properties of Silicate Melts. Reviews in Mineralogy. Vol 32. Mineralogical Society of America

Suk NI (1998) Distribution of ore elements between immiscible liquids in silicate – phosphate systems (experimental investigation). Acta Univ Carol Geol 42:138–140

Switzer GS (1975) Composition of three glass phases present in an Apollo 15 basalt fragment. *In*: Mineral Sciences Investigations 1972-1973. Smithsonian Contribution to Earth Sciences Vol 14. Switzer GS (ed), Smithsonian Institution Press, p 25-30

Taylor JR, Dinsdale AT (1990) Thermodynamic and phase diagram data for the CaO-SiO_2 system. Calphad 14:71-88

Tewhey JD, Hess PC (1979) 2-Phase region in the CaO-SiO_2 system: experimental data and thermodynamic analysis. Phys Chem Glasses 20:41-53

Thibault Y, Edgar AD, Lloyd FE (1992) Experimental investigation of melts from a carbonated phlogopite lherzolite: implications for metasomatism in the continental lithospheric mantle. Am Mineral 77:784-794

Thompson JB Jr, Thompson AB (1976) A model system for mineral facies in pelitic schists. Contrib Mineral Petrol 58:243-277

Tien TY, Hummel FA (1962) The system SiO_2-P_2O_5. J Am Ceram Soc 45:422-424

Tuttle OF, Bowen NL (1950) High temperature albite and contiguous feldspars. J Geology 58:572-583

Tuttle OF, Bowen NL (1958) Origin of granite in the light of experimental studies in the system $NaAlSi_3O_8$-$KAlSi_3O_8$-SiO_2-H_2O. Geol Soc Am Mem 74:1-153

Veksler IV (2004) Liquid immiscibility and its role at the magmatic-hydrothermal transition: a summary of experimental studies. Chem Geol 210:7-31

Veksler IV, Dorfman AM, Dingwell DB, Zotov N (2002a) Element partitioning between immiscible borosilicate liquids: a high-temperature centrifuge study. Geochim Cosmochim Acta 66:2603–2614

Veksler IV, Fedorchuk YM, Nielsen TFD (1998a) Phase equilibria in the silica -undersaturated part of the$KAlSiO_4$–Mg_2SiO_4–Ca_2SiO_4–SiO_2–F system at 1 atm and the larnite-normative trend of melt evolution. Contrib Mineral Petr 131:347-363

Veksler IV, Petibon C, Jenner G, Dorfman AM, Dingwell DB (1998b) Trace element partitioning in immiscible silicate and carbonate liquid systems: an initial experimental study using a centrifuge autoclave. Journal of Petrology 39:2095-2104

Veksler IV, Thomas R, Schmidt C (2002b) Experimental evidence of three coexisting immiscible fluids in synthetic granite pegmatite. Am Mineral 87:775–779

Visser W, Koster van Groos AF (1979a) Effect of pressure on liquid immiscibility in the system K_2O-FeO-Al_2O_3-SiO_2-P_2O_5. Am J Sci 279:1160-1175

Visser W, Koster van Groos AF (1979b) Effects of P_2O_5 and TiO_2 on liquid-liquid equilibria in the system K_2O-FeO-Al_2O_3-SiO_2. Am J Sci 279:970-988

Visser W, Koster van Groos AF (1979c) Phase relations in the system K_2O-FeO-Al_2O_3-SiO_2 at 1 atmosphere with special emphasis on low temperature liquid immiscibility. Am J Sci 279:70-91

Waldbaum DR, Thompson JB Jr (1969) Mixing properties of sanidine crystalline solution. IV. Phase diagrams from equations of state. Am Mineral 54:1274-1298

Watson EB (1976) Two-liquid partition coefficients: Experimental data and geochemical implications. Contrib Mineral Petrol 56:119-134

Webster JD, DeVivo B (2002) Experimental and modeled solubilities of chlorine in aluminosilicate melts, consequences of magma evolution, and implications for exsolution of hydrous chloride melt at Mt. Somma-Vesuvius. Am Mineral 87:1046-1061

Weiblen PW, Roedder E (1973) Petrology of melt inclusions in Apollo samples 15598 and 62295, and of clasts in 67915 and several lunar soils. Proc Fourth Lunar Sci Conf, Geochim Cosmochim Acta Suppl 4:681-703

White J, Howatt DD, Hay R (1934) The binary system MnO-SiO_2. J Royal Tech Coll (Glasgow) 3:231-240

Wu P, Eriksson G, Pelton AD, Blander M (1993) Prediction of the thermodynamic properties and phase diagrams of silicate systems: evaluation of the FeO-MgO-SiO_2 System. Isij Int 33:26-35

Wyllie PJ (1977) Mantle fluid compositions buffered by carbonates in peridotite-CO_2-H_2O. J Geol 85:187-207

Wyllie PJ (1978) Mantle fluid compositions buffered in peridotite-CO_2-H_2O by carbonates, amphibole, and phlogopite. J Geol 86:687-713

Wyllie PJ (1987) Volcanic rocks: boundaries from experimental petrology. Fortschr Mineral 65:249-284

Wyllie PJ (1989) Origin of carbonatites: evidence from phase equilibrium studies. *In*: Carbonatites. Genesis and Evolution. Bell K (ed) Unwin Hyman, p 500-545

Wyllie PJ, Huang WL (1976) Carbonation and melting reactions in system CaO-MgO-SiO_2-CO_2 at mantle pressures with geophysical and petrological applications. Contrib Mineral Petrol 54:79-107

Yoder HSJ, Stewart DB, Smith JV (1957) Ternary feldspars. Carnegie I Wash 56:206-214

Yoder HSJ, Tilley CE (1962) Origin of basalt magmas: an experimental study of natural and synthetic rock systems. J Petrol 3:342-53